AWARD NUMBER: W81XWH-16-1-0197

TITLE: Directly Conjugated Single-Domain VHHs Targeting MHC Class II Prime T-Cell Responses Against Pancreatic Cancer Neoantigens

PRINCIPAL INVESTIGATOR: Dr. Stephanie Dougan

CONTRACTING ORGANIZATION: Dana-Farber Cancer Institute

REPORT DATE: January 2020

TYPE OF REPORT: Final report

PREPARED FOR: U.S. Army Medical Research and Development Command
Fort Detrick, Maryland 21702-5012

REPORT DOCUMENTATION PAGE

Form Approved
OMB No. 0704-0188

1. REPORT DATE	2. REPORT TYPE	3. DATES COVERED
Jan 2020	Final	09/30/2016 - 09/29/2019

4. TITLE AND SUBTITLE

Directly Conjugated Single-Domain VHHs Targeting MHC Class II Prime T-Cell Responses Against Pancreatic Cancer Neoantigens

5a. CONTRACT NUMBER
W81XWH-16-1-0197

5b. GRANT NUMBER

5c. PROGRAM ELEMENT NUMBER

6. AUTHOR(S)

Stephanie Dougan, Dana-Farber Cancer Institute

Stephanie_dougan@dfci.harvard.edu

5d. PROJECT NUMBER

5e. TASK NUMBER

5f. WORK UNIT NUMBER

7. PERFORMING ORGANIZATION NAME(S) AND ADDRESS(ES)
Dana-Farber Cancer Institute
450 Brookline Avenue
Boston, MA 02215-5450

8. PERFORMING ORGANIZATION REPORT NUMBER

9. SPONSORING / MONITORING AGENCY NAME(S) AND ADDRESS(ES)

U.S. Army Medical Research and Development Command
Fort Detrick, Maryland 21702-5012

10. SPONSOR/MONITOR'S ACRONYM(S)

11. SPONSOR/MONITOR'S REPORT NUMBER(S)

12. DISTRIBUTION / AVAILABILITY STATEMENT

Approved for Public Release; Distribution Unlimited

13. SUPPLEMENTARY NOTES

14. ABSTRACT
Background: Pancreatic cancer is one of the deadliest cancers, with a 5 year survival rate of 5%. The exceptionally poor prognosis of this disease can be traced to several factors. Located in a vital region of the body, the majority of primary pancreatic tumors are inoperable and rapidly metastatic. Furthermore, pancreatic cancers are dense, fibrotic masses that preclude adequate drug delivery. Immunotherapy has shown impressive clinical benefit for other cancers, particularly for metastatic melanoma. Since immunotherapy targets the immune system, and not a particular type of cancer, these new drugs were originally hoped to be applicable across all tumor types as a pan-cancer medication. However, pancreatic cancer was among the cancer types in which immunotherapy has largely failed. We propose a novel strategy of using an alpaca single domain antibody against MHC class II to activate CD4 T cells against pancreatic cancer specific neoantigens. T cell activation would occur outside the tumor, in lymph nodes and spleen; our hope is that these activated T cells would then infiltrate the pancreatic mass and cause tumor rejection.

15. SUBJECT TERMS
Pancreatic cancer, cancer vaccine, neoantigen, MHC class II, alpaca single-domain antibodies

16. SECURITY CLASSIFICATION OF:			17. LIMITATION OF ABSTRACT	18. NUMBER OF PAGES	19a. NAME OF RESPONSIBLE PERSON
a. REPORT	b. ABSTRACT	c. THIS PAGE			USAMRMC
Unclassified	Unclassified	Unclassified	Unclassified		19b. TELEPHONE NUMBER *(include area code)*

TABLE OF CONTENTS

Introduction

Pancreatic cancer is one of the deadliest cancers, with a 5 year survival rate of 5%. The exceptionally poor prognosis of this disease can be traced to several factors. Located in a vital region of the body, the majority of primary pancreatic tumors are inoperable and rapidly metastatic. Furthermore, pancreatic cancers are dense, fibrotic masses that preclude adequate drug delivery. Immunotherapy has shown impressive clinical benefit for other cancers, particularly for metastatic melanoma. Since immunotherapy targets the immune system, and not a particular type of cancer, these new drugs were originally hoped to be applicable across all tumor types as a pan-cancer medication. However, pancreatic cancer was among the cancer types in which immunotherapy has largely failed. We propose a novel strategy of using an alpaca single domain antibody against MHC class II to activate CD4 and CD8 T cells against pancreatic cancer specific antigens. T cell activation would occur outside the tumor, in lymph nodes and spleen; our hope is that these activated T cells would then infiltrate the pancreatic mass and cause tumor rejection. This fundamentally new type of vaccination strategy could be applied to many kinds of cancers, and also implemented as part of combination immunotherapy regimens for pancreatic cancer.

Keywords

Pancreatic cancer immunotherapy, vaccines, vaccine design, alpaca VHH, MHC class II, neoantigens, adjuvant, CD4 T cells, CD8 T cells

Accomplishments

What were the major goals of the project?

List the major goals of the project as stated in the approved SOW. If the application listed milestones/target dates for important activities or phases of the project identify these dates and show actual completion dates or the percentage of completion.

Determine putative antigens for KPC cell lines

Sub-Task 1A: Exome sequencing of KPC cell lines and prediction of neoantigens

We performed RNAseq on both Panc02 and KPC cells. RNAseq was chosen over exome sequencing because we could extract both neoantigens and their expression levels from the same dataset. We have completed our neoantigen predictions for the KPC line, and selected the top 10 most likely candidates for further validation.

Sub-Task 1B: Validation of epitopes in vitro.

We immunized mice with 10 DC-15 neoantigen constructs and evaluated the T cell response ex vivo by IFNg ELISA, by flow cytometry, and by ELISpot.

Sub-Task 1C: Validation of epitopes in vivo.

We used pooled neoantigens and showed very modest ability to vaccinate against challenge with KPC pancreatic tumors. We attempted to further optimize by adding CpG adjuvant and by optimizing the route/dose of vaccination. Neither approach was successful for pancreatic cancer.

Develop DC15 neoantigen conjugates

Sub-Task 2A: Construction of DC15 conjugates.

We developed a robust pipeline for generating DC15 conjugated to both peptides and CpG. These reagents were completed for DC15-SIINFEKL, DC15-TRP1, and for 10 KPC neoantigens in adequate quantities for in vivo studies.

Sub-Task 2B: Validation of DC15 conjugates in vitro.

We completed this task. We determined that finding the relevant MHC class II expressing cell in vivo was important for understanding vaccine efficacy, and so we expanded this task slightly to include evaluation of DC15 conjugates in mice lacking B cells, cross-presenting DCs, or b2m as a negative control. We determined that DC15-conjugates induced CD8 T cell responses in mice lacking B cells but not in mice lacking b2m, indicating that cross-presenting DCs are the likely relevant antigen presenting cell in vivo.

Test DC15 conjugates in vivo

Sub-Task 3A: Determine efficacy of drug(s) in orthotopic pancreatic cancer model.

We unfortunately showed a lack of efficacy of pooled neoAg vaccines in pancreatic cancer models, but were able to show induction of tetramer+ CD8 T cells in a melanoma model in combination with an IL-2 mimetic (Neo2/15).

Sub-Task 3B: Determine immune correlates of efficacy.

We demonstrated that induction of antigen-specific CD8 T cells (identified by tetramer staining) was correlated with efficacy.

What was accomplished under these goals?

Subtask 1A: We generated a list of predicted MHC class I presented model neoantigens expressed by KPC cells, and selected 11 candidates for initial in vivo testing based on their expression level in tumor cells and their MHC binding scores (Table 1).

Table 1: Predicted model neoantigens from KPC cell line

	allele	peptide (8/9)	percentile_rank	Gene	Mean Expression	wt peptide sequence
Neo1	H-2-Db	NMIEAGDAL	1.5	Lars	6943	NMIDAGDAL
Neo2	H-2-Kb	VSALSSRV	1.75	Hjurp	3608	VSALSSRG
Neo3	H-2-Db	RALRKQQPI	0.2	Smcr8	1838	AAVSGLVAL
Neo4	H-2-Db	VSIPPQSYI	1.3	Smcr8	1838	Premature Start Codon
Neo5	H-2-Kb	TGLRFHEL	0.24	Kntc1	1712	TGLWFHEL
Neo6	H-2-Kb	MSYRFRQE	0.17	Cdt1	1711	TSYRFRQE
Neo7	H-2-Db	GQIKTVYPM	0.9	Cdt1	1711	GQIKTVYPT
Neo8	H-2-Db	EMFHSMDTI	2	Cdt1	1711	EMFHSRDTI
Neo9	H-2-Db	PSLLMVVAL	1.9	Slc9a1	954	PSLLVVVAL
Neo10	H-2-Kb	SGVLPASL	1.7	Gadd45gip1	938	SPPRYATL
Neo11	H-2-Kb	KLRTYVTL	1.7	Ppp1r21r	745	KLQTYVTL

Subtask 2A: These peptides were generated in large quantity as DC15 and control VHH (96G3m) conjugates thanks to a robust production pipeline. Neo8 and Neo9 peptide synthesis was suboptimal, and these did not conjugate well to the VHHs. We therefore dropped Neo8 and Neo9 from subsequent analysis.

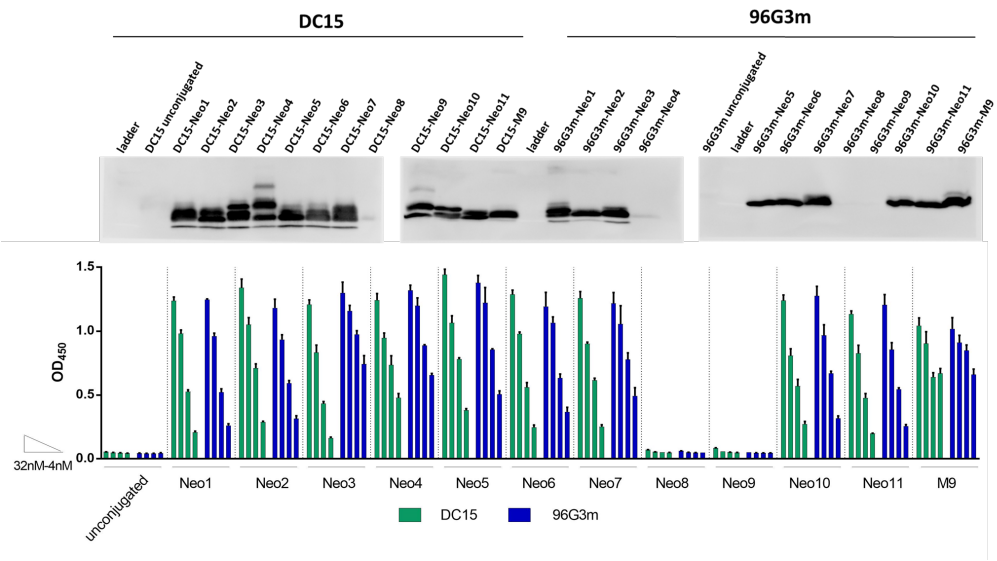

Figure 1: GGG-Neoantigen peptides were conjugated to LPETG-tagged DC15 (anti-MHCII VHH) or 96G3m (control VHH) using sortase. Peptides were synthesized with a biotin tag, and conjugates were normalized to the amount of incorporated biotin as detected by anti-biotin ELISA.

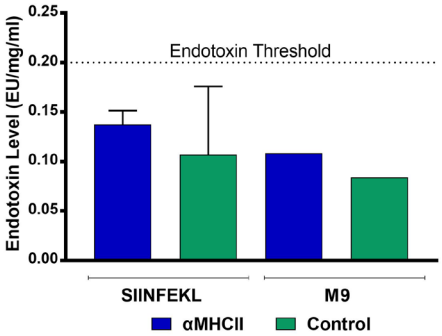

Figure 2: All VHH-peptide conjugates are purified by FPLC and washed extensively to remove residual endotoxin. Endotoxin levels were confirmed to be below a minimum threshold of 0.2 EU/mL. This is part of our production pipeline quality control.

Subtask 1B: Mice were vaccinated via footpad injection, boosted 14 days later, then spleens and popliteal draining lymph nodes were harvested. To evaluate whether each peptide generated a T cell response, spleen and LN cells were analyzed by 1) restimulation with BMDCs pulsed with the cognate neoAg peptide, followed by IFNg ELISA; 2) restimulation with BMDCs pulsed with the cognate neoAg peptide, followed by staining for activation markers CD69 and PD-1 and analysis by flow cytometry. These results showed that neoAg responses were undetectable by flow cytometry due to high background expression of activation markers, but IFNg ELISA was promising for neoantigens 1, 2, 3, 4, 6, 7, 10 and 11.

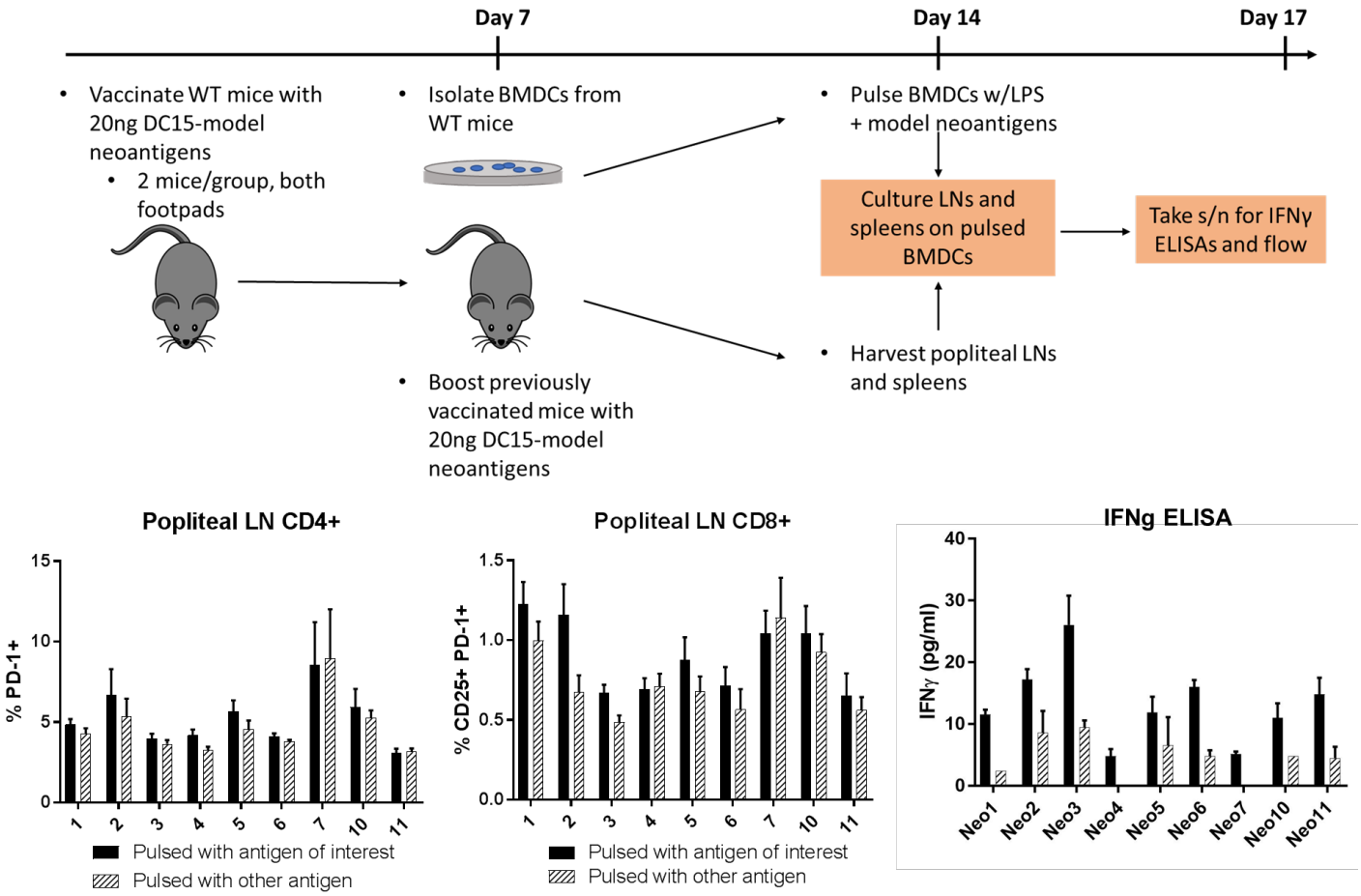

Figure 3: Mice were vaccinated according to the scheme as shown. Bottom panels show flow cytometry and IFNg ELISA results from draining lymph node cells of vaccinated mice. Each group of cells was simulated with the neoantigen used for vaccination (solid bars) and an irrelevant control antigen (dashed bars) as a specificity control.

Subtask 1C: Mice were vaccinated with all 9 successfully produced DC15 neoAg conjugates as a pooled vaccine via footpad injection and boosted 14 days later. Control mice were vaccinated with an equimolar amount of DC15 without peptide. Mice were challenged with subcutaneous KPC tumors on the flank, and tumor growth was measured over time. All control mice developed tumors, while 9/10 vaccinated mice developed tumors. One vaccinated mouse survived tumor-free.

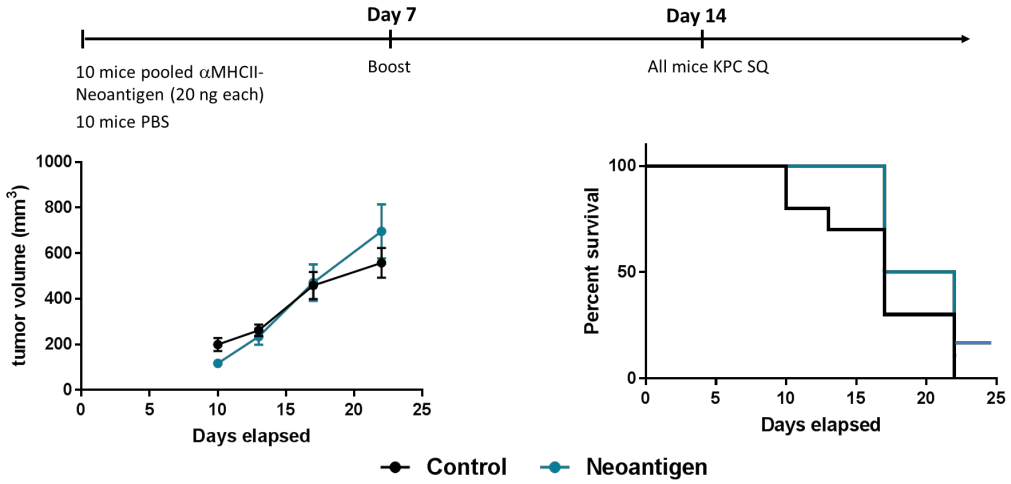

Figure 4: Mice were vaccinated with DC15 only, or with all DC15-neoAg conjugates pooled, according to the diagram shown. Tumor size and survival were measured over time.

Subtask 2B: To determine the MHC class II antigen presenting cell required for efficacy of this vaccination strategy, we used two peptides for which CD8 T cells specific for those antigens were available, namely OT-I T cells and SIINFEKL, and TRP1 T cells and M9 peptide. We generated DC15 and 96G3m conjugated versions of each peptide, then vaccinated wild type mice or muMt-/- mice (lacking B cells), and b2m-/- mice (lacking MHC class I, negative control) to determine whether B cells are required for DC15-enhanced antigen presentation. These experiments will also be performed in Batf3-/- mice (lacking cross-presenting dendritic cells)

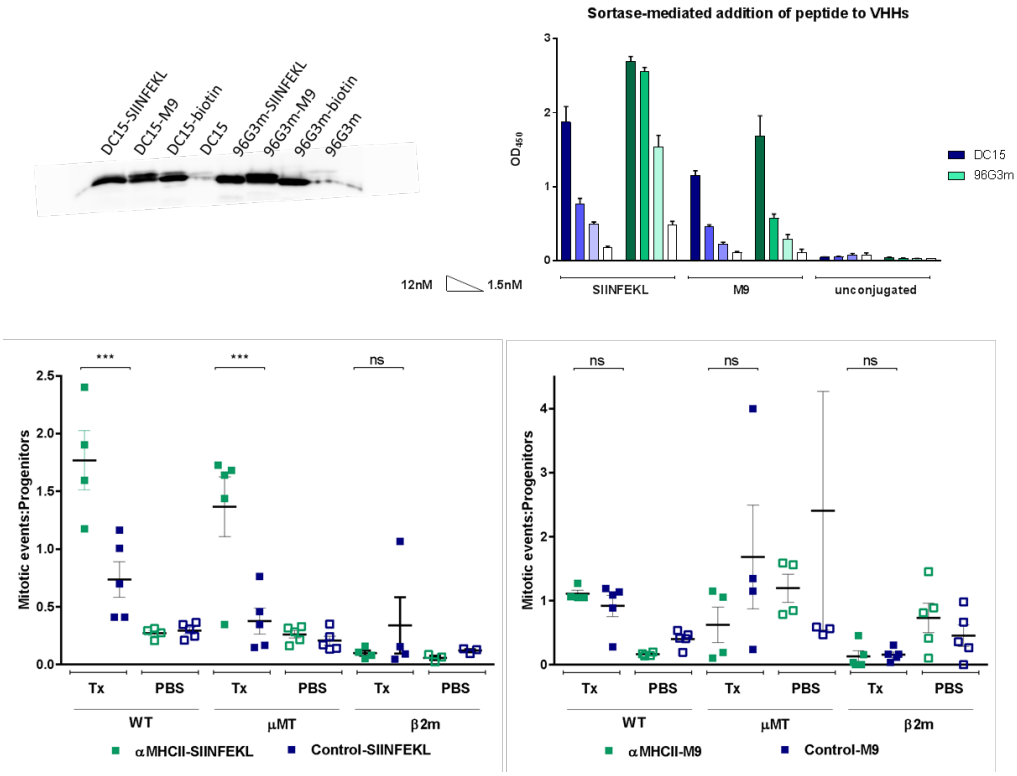

Figure 5: DC15-SIINFEKL and DC15-M9 conjugates were produced and concentrations normalized based on the amount of biotin signal detected in the conjugated material. Bottom panels show mice of the indicated genotypes vaccinated in the footpads with DC15 (aMHCII) or 96G3m (Control) conjugates. Mice also received adoptive transfer of CFSE-labeled OT-I or TRP1 CD8 T cells. T cell proliferation was measured by flow cytometry of draining lymph nodes 72 hours post vaccination.

Subtask 3A/B: From the one surviving mouse in our tumor challenge experiment, we performed an ELISpot analysis from draining lymph node and spleen restimulated with KPC tumor cells. Titrated TRP1 cells activated with B16 tumor cells were included as a positive control and standard curve (Figure 6).

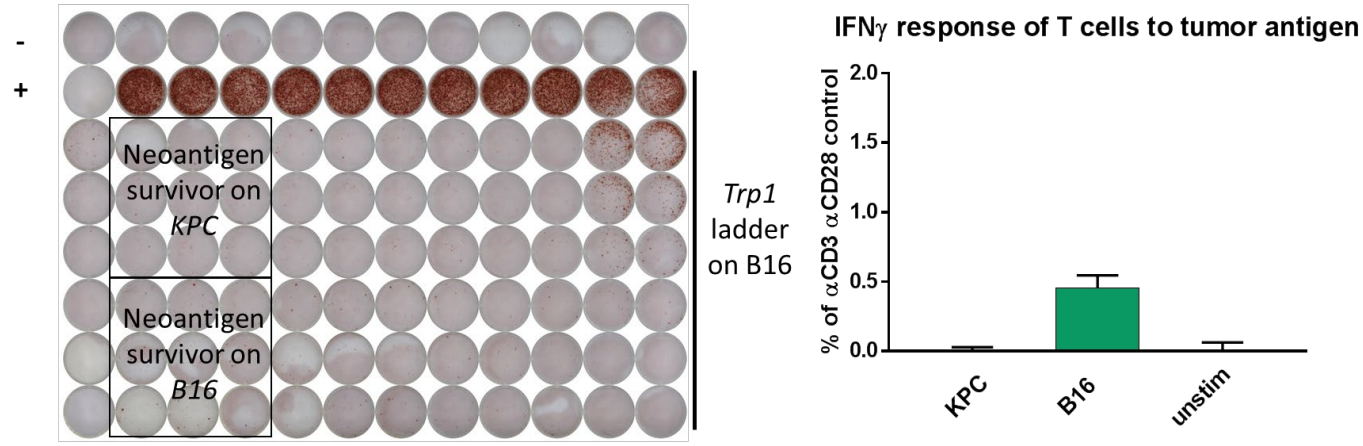

Figure 6: Draining lymph node cells from the surviving mouse from Figure 4 were plated into and ELISpot plate coated with IFNg pretreated KPC tumor cells and the irrelevant tumor B16. B16-specific T cells (TRP1) were titrated and included to define the limit of detection of this assay.

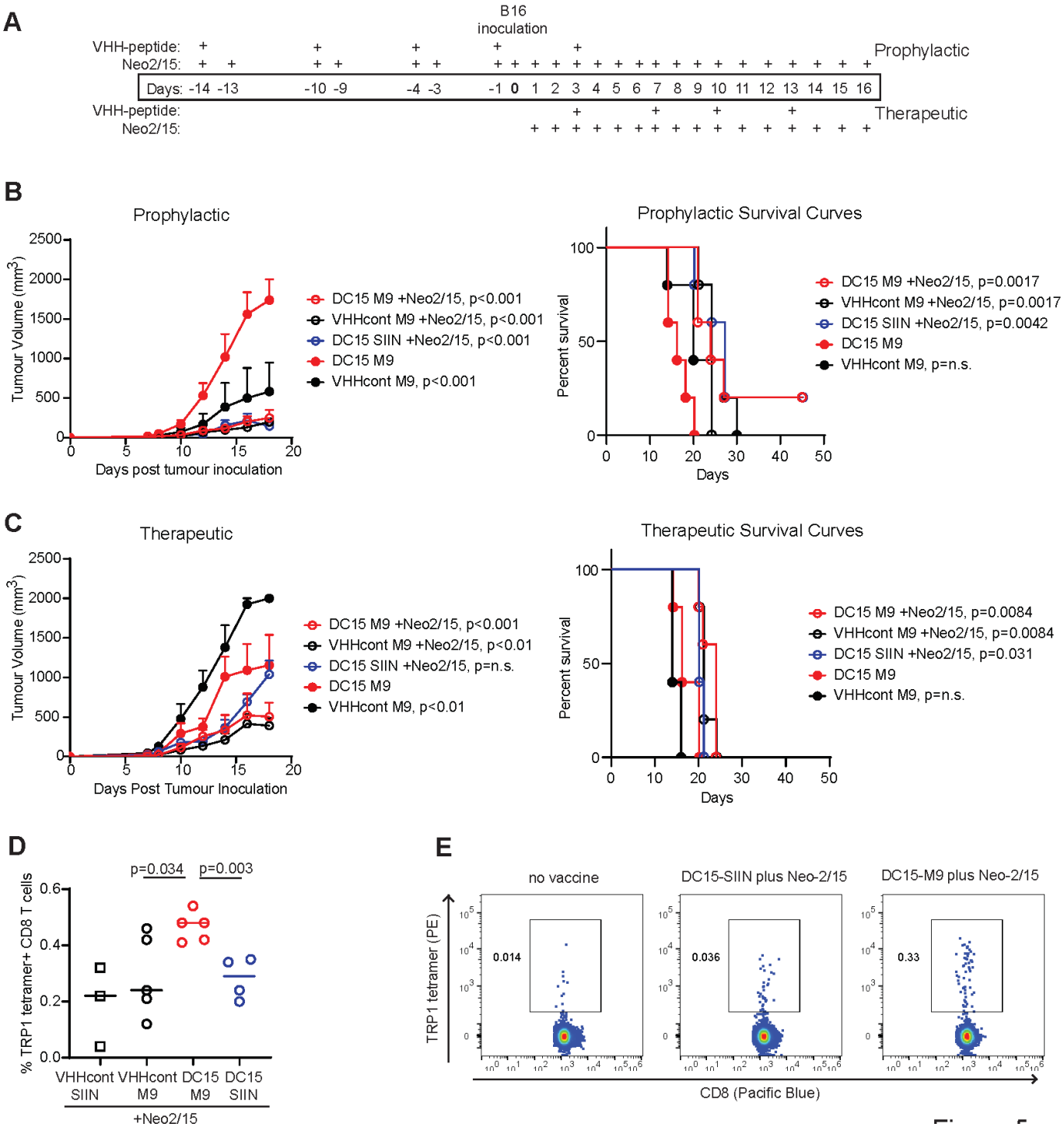

Figure 7: Combination of DC15 based vaccination and Neo2/15 leads to anti-tumor immunity in the B16 melanoma model. A) Schedule of treatments for prophylactic and therapeutic experimental cohorts. Neo2/15 was used at 10µg per dose; VHH-peptides were used at 10ng per dose. M9 peptide was used as the relevant antigenic epitope; SIINFEKL was included as a negative control. N=5 mice per group. Experiments were conducted in parallel such that all mice were inoculated subcutaneously with 250,000 B16 cells on the same day. B) Tumor growth and survival of mice in the prophylactic cohorts. P values shown are comparisons to the DC15-M9 vaccinated group. C) Tumor growth and survival of mice in the therapeutic cohorts. P values shown are comparisons to the DC15-M9 vaccinated group. D) C57BL/6 mice were vaccinated with 10ng per dose of VHH-peptide on Days 0 and 4. Mice received 10µg per mouse Neo2/15 daily staring on day 0. Draining lymph nodes were harvested on day 9, stained and analyzed by flow cytometry. E) C57BL/6 mice were inoculated with B16 tumors and left untreated. When tumors reached >1cm3, draining lymph node cells were harvested from mice with progressively growing tumors as well as from the single surviving mice in the DC15-SIIN/Neo2/15 and DC15-M9/Neo2/5 prophylactic cohorts shown in B. Cells were stained with anti-CD8 and TRP1 tetramers. Flow cytometry plots are gated on total CD8+ cells.

What opportunities for training and professional development has the project provided?

- Mr. Patrick Bruck finished his training in my lab, and began his PhD studies at the University of California San Diego.
- Ms. Stephanie Crowley finished her training in my lab, and began her PhD studies at Washington University in St. Louis.
- Dr. Hee-Jin Jeong worked on this project as part of her training in my lab. She accepted an offer from Hongik University (South Korea) and is now an Assistant Professor leading her own group.

How were the results disseminated to communities of interest?

- A paper describing these findings is currently in press in Open Biology, an open access scientific journal. The page proofs are attached to this report.

What do you plan to do during the next reporting period to accomplish the goals?

We have successfully completed this project.

Impact

Describe distinctive contributions, major accomplishments, innovations, successes, or any change in practice or behavior that has come about as a result of the project relative to:

What was the impact on the development of the principal discipline(s) of the project?

- A paper describing these findings is currently in press in Open Biology, an open access scientific journal. The page proofs are attached to this report. This paper will be read by members of the pancreatic cancer community, and also scientists in other disciplines.

What was the impact on other disciplines?

- A paper describing these findings is currently in press in Open Biology, an open access scientific journal. The page proofs are attached to this report. This paper will be read by members of the pancreatic cancer community, and also scientists in other disciplines.
- I also served as a Scientist Reviewer for the CDMRP DoD peer-review panel (Melanoma, PB) in 2020.

What was the impact on technology transfer?

- Nothing to report
-

What was the impact on society beyond science and technology?

- For Mr. Patrick Bruck and Ms. Stephanie Crowley especially, this project has been an invaluable training experience as they prepared for graduate school. I believe that one of the major goals of my lab is to foster scientific appreciation and education in the next generation, and direct one-on-one mentorship can change the course of a person's life.
- On a broader level, I am the course director for a summer science program for undergraduates, which aims to expose students to immunology research at Harvard. Our website is: http://dms.hms.harvard.edu/immunology/prospective_students/summer_program.html. I also developed a new Immunology curriculum for third year Harvard Medical School students.

Changes/Problems

Changes in approach and reasons for change
We realized that CpG was not a good adjuvant, and so we switched to using Neo2/15, as recently published: Silva DA, Yu S, Ulge U, Spangler JB, Jude KM, Labao-Almeida C, Ali LR, Quijano-Rubo A, Ruterbusch M, Leung I, Biary T, Crowley S, Marco E, Walkey CD, Weitzner BD, Pardo-Avila F, Carter L, Stewart L, Riddell S, Pepper M, Bernardes GJL, Dougan M, Garcia KC, Baker D. De novo design of potent and selective mimics of IL-2/IL-15. Nature. 2019 Jan;565(7738):186-191.

Actual or anticipated problems or delays and actions or plans to resolve them
none

Changes that had a significant impact on expenditures
n/a

Significant changes in use or care of human subjects, vertebrate animals, biohazards, and/or select agents
n/a

Products

Publications, conference papers, and presentations
Journal publications

Crowley SJ*, Bruck PT*, Bhuiyan MA, Mitchell-Gears A, Walsh MJ, Zhangxu K, Ali LR, Jeong H-J, Ingram JR, Knipe DM, Ploegh HL, Dougan M, Dougan SK. Neoleukin-2 enhances anti-tumor immunity downstream of peptide vaccination targeted by an anti-MHC class II VHH. in press *Open Biology*.

Books or other non-periodical, one-time publications
none

Other publications, conference papers, and presentations
1. Balachandran VP, Beatty GL, **Dougan SK**. Broadening the impact of immunotherapy to pancreatic cancer: Challenges and opportunities. Gastroenterology. 2019 Jan 17.
2. Dougan M, Dranoff G, **Dougan SK**. Cancer Immunotherapy: Beyond Checkpoint Blockade. Annual Review of Cancer Biology. March 2019. Vol. 3:55-75.
3. Dougan M, Dranoff G, **Dougan SK**. GM-CSF, IL-3, and IL-5 Family of Cytokines: Regulators of Inflammation. Immunity. 2019 Apr 16;50(4):796-811.
4. **Dougan SK**, Dougan M. SMAC mimetics throw a molecular switch to control TH17 responses. Sci Signal. 2019 Aug 27;12(596).
5. Dougan M, **Dougan SK**. Programmable bacteria as cancer therapy. Nat Med. 2019 Jul;25(7):1030-1031.

2017	Targeting immunotherapy to the tumor microenvironment Pew Foundation Scientific Annual meeting, Santa Barbara, CA
2017	Targeting immunotherapy to the tumor microenvironment, invited oral presentation EACR-AACR-SIC special conference From Cancer Biology to the Clinic Florence, Italy
2017	Targeting immunotherapy to the tumor microenvironment, Invited oral presentation 3rd International CRCL Symposium Lyon, France

Website(s) or other Internet site(s)

Dougan lab website: http://douganlab.dana-farber.org/

Technologies or techniques
None

Inventions, patent applications, and/or licenses
None

Other Products
None

Participants and Other Collaborating Organizations

What individuals have worked on the project?

Name:	Dr. Stephanie Dougan
Project Role:	Principal Investigator
Researcher Identifier (e.g. ORCID ID):	N/A
Nearest person month worked:	3.00
Contribution to Project:	Dr. Dougan was responsible for the conception and design of all the studies. She supervised their execution, analyzed data, and presented the findings to the scientific community.
Funding Support:	N/A

Name:	Dr. Max Heckler
Project Role:	Postdoctoral Fellow
Researcher Identifier (e.g. ORCID ID):	N/A
Nearest person month worked:	3.0
Contribution to Project:	Dr. Heckler has expertise in pancreatic cancer clinical care, and has become proficient in orthotopic tumor injections in mice. He managed all surgical implantation of pancreatic tumors, analyzed data, and contributed to project experiments.
Funding Support:	N/A

Name:	Patrick Bruck
Project Role:	Research Technician
Researcher Identifier (e.g. ORCID ID):	N/A

Nearest person month worked:	2.0
Contribution to Project:	Mr. Bruck performed in vitro cell culture assays and in vivo mouse studies.
Funding Support:	N/A

Name:	Katherine Ventre
Project Role:	Research Technician
Researcher Identifier (e.g. ORCID ID):	N/A
Nearest person month worked:	2.0
Contribution to Project:	Ms. Ventre assisted Dr. Heckler in vitro cell culture assays and in vivo mouse studies, as well as analysis of transcriptional data.
Funding Support:	N/A

Name:	Stephanie Crowley
Project Role:	Research Technician
Researcher Identifier (e.g. ORCID ID):	N/A
Nearest person month worked:	3.0
Contribution to Project:	Ms. Crowley assisted Dr. Heckler in vitro cell culture assays and in vivo mouse studies, as well as analysis of transcriptional data.
Funding Support:	N/A

Name:	Rafael Recio
Project Role:	Research Operations Assistant
Researcher Identifier (e.g. ORCID ID):	N/A
Nearest person month worked:	0.0
Contribution to Project:	Mr. Recio carried out all cleaning and decontamination of laboratory glassware, autoclaving waste, and making sterile liquid media for bacterial cultures for the Dougan lab. He also assisted with receiving, stocking and autoclaving of media.
Funding Support:	N/A

Has there been a change in the active other support of the PD/PI(s) or senior/key personnel since the last reporting period?

Project Number N/A (Wolpin) 08/01/2018-07/31/2019 0.60 CM
Hale Center Initiative $150,000
“Reprogramming macrophages in pancreatic cancer with Erk5 inhibitors”

The goal of this collaboration project is to examine Erk5i as part of a combination immunotherapy for pancreatic cancer.
Change: Award extended

What other organizations were involved as partners?
None

Organization Name:

- N/A

SPECIAL REPORTING REQUIREMENTS

None

-

OPEN BIOLOGY

royalsocietypublishing.org/journal/rsob

Research

Cite this article: Crowley SJ *et al*. 2020 Neoleukin-2 enhances anti-tumour immunity downstream of peptide vaccination targeted by an anti-MHC class II VHH. *Open Biol.* **10**: 190235.
http://dx.doi.org/10.1098/rsob.190235

Received: 27 September 2019
Accepted: 6 January 2020

Subject Area:
immunology

Keywords:
VHH, cancer vaccines, cytokines, cancer immunology, neoantigens, alpaca nanobodies

Author for correspondence:
Stephanie K. Dougan
e-mail: stephanie_dougan@dfci.harvard.edu

†These authors contributed equally to this study.
‡Deceased 18 April 2018.

THE ROYAL SOCIETY PUBLISHING

Neoleukin-2 enhances anti-tumour immunity downstream of peptide vaccination targeted by an anti-MHC class II VHH

Stephanie J. Crowley[1,†], Patrick T. Bruck[1,†], Md Aladdin Bhuiyan[1,2], Amelia Mitchell-Gears[1,3], Michael J. Walsh[4], Kevin Zhangxu[1], Lestat R. Ali[1], Hee-Jin Jeong[1,6], Jessica R. Ingram[1,‡], David M. Knipe[4], Hidde L. Ploegh[7], Michael Dougan[2] and Stephanie K. Dougan[1,5]

[1]Department of Cancer Immunology and Virology, Dana-Farber Cancer Institute, Boston, MA, USA
[2]Department of Medicine, Division of Gastroenterology, Massachusetts General Hospital and Harvard Medical School, Boston, MA, USA
[3]University of Leeds, Leeds, West Yorkshire, UK
[4]Program in Virology and Department of Microbiology, and [5]Department of Immunology, Harvard Medical School, Boston, MA, USA
[6]Department of Biological and Chemical Engineering, Hongik University, Mapo-gu, Seoul, Korea
[7]Program in Cellular and Molecular Medicine, Boston Children's Hospital, Boston, MA, USA

DMK, 0000-0003-1554-6236; SKD, 0000-0002-2263-363X

Cancer-specific mutations can lead to peptides of unique sequence presented on MHC class I to CD8T cells. These neoantigens can be potent tumour-rejection antigens, appear to be the driving force behind responsiveness to anti-CTLA-4 and anti-PD1/L1-based therapies and have been used to develop personalized vaccines. The platform for delivering neoantigen-based vaccines has varied, and further optimization of both platform and adjuvant will be necessary to achieve scalable vaccine products that are therapeutically effective at a reasonable cost. Here, we developed a platform for testing potential CD8T cell tumour vaccine candidates. We used a high-affinity alpaca-derived VHH against MHC class II to deliver peptides to professional antigen-presenting cells. We show *in vitro* and *in vivo* that peptides derived from the model antigen ovalbumin are better able to activate naive ovalbumin-specific CD8T cells when conjugated to an MHC class II-specific VHH when compared with an irrelevant control VHH. We then used the VHH-peptide platform to evaluate a panel of candidate neoantigens *in vivo* in a mouse model of pancreatic cancer. None of the candidate neoantigens tested led to protection from tumour challenge; however, we were able to show vaccine-induced CD8T cell responses to a melanoma self-antigen that was augmented by combination therapy with the synthetic cytokine mimetic Neo-2/15.

1. Introduction

CD8T cells can recognize tumours via cancer antigens presented on MHC class I. These cancer antigens come in several categories, including developmental or tissue-restricted antigens, self-antigens with altered post-translational modifications and viral antigens in the case of viral-associated cancers [1]. In addition, mutations acquired during the process of oncogenesis can lead to altered peptide sequences presented on MHC class I and class II. These so-called neoantigens can be potent tumour-rejection antigens and appear to be the driving force behind responsiveness to anti-CTLA-4 and anti-PD1/L1-based therapies [2,3]. Given the unique specificity for tumour versus healthy tissue and the lower degree of

tolerance induction, neoantigen-based vaccines are currently in clinical trials for several types of advanced malignancies [4]. The platform for delivering neoantigen-based vaccines has varied, with both RNA and synthetic long peptides being equally effective in small-scale trials [5–8]. The adjuvants used have been largely empirical and have been selected based on safety profile and availability rather than optimal stimulation of tumour-specific CD8T cell responses. Further optimization of both platform and adjuvant will be necessary to achieve scalable vaccine products that are therapeutically effective at a reasonable cost [9].

Recently activated T cells require IL-2 signalling to sustain their growth and proliferation [10]. Recombinant IL-2 is approved as a therapy for melanoma but is limited by severe systemic toxicity and the preferential induction of proliferation of Foxp3+ regulatory T cells (Tregs) that express the high-affinity IL2Rα chain CD25 [11]. High-dose IL-2 is required to overcome the sink effect of Treg-expressed CD25; however, these doses induce severe systemic side effects requiring hospitalization [12]. Structural variants of IL-2 that selectively bind the IL2Rβγ complex without binding to IL2Rα have been developed, although like naturally occurring cytokines, these variants suffer from limited thermal stability [13–16]. A synthetically designed protein called Neoleukin-2 (Neo-2/15) was reported to exclusively bind IL2Rβγ without binding to IL2Rα [17]. This engineered cytokine displayed improved thermal stability and was able to induce T-cell proliferation *in vitro* even after boiling the cytokine for an hour [17]. Neo-2/15 augmented the therapeutic efficacy of the melanoma-specific antibody TA99 in a preclinical model and had a lower toxicity profile compared with recombinant murine IL-2 [17]. We, therefore, tested whether Neo-2/15 could be used to augment peptide vaccine-induced CD8T cell responses in a similar model.

Most conventional vaccine strategies elicit neutralizing antibody responses but fail to generate antigen-specific CD8T cells. To prime naive T-cell responses, the antigen must be expressed by or targeted to a professional antigen-presenting cell (APC). Several methodologies have been used to address this challenge including injection of DNA or RNA into the skin, use of live viral vectors or loading of dendritic cells *ex vivo*. Delivery of antigen to professional APCs can also be achieved by targeting unique cell surface receptors. To this end, we reasoned that MHC class II is constitutively expressed on professional APCs and is endocytosed, leading to localization of bound cargo to the endolysosomal compartment [18,19]. Alpaca nanobody fragments (VHHs) against MHC class II have been used to target antigenic cargo for endocytic processing and presentation on MHC class II to CD4T cells [19–21]. Although cross-presentation of these same cargos on MHC class I for activation of CD8T cells was somewhat limited, the lower degree of CD8T cell priming could reflect the modest affinity of the anti-MHC class II VHH7 for its target [19,22]. DC15 is a VHH specific for MHC class II that binds with fivefold higher affinity than VHH7 and can competitively inhibit VHH7 binding to its target [22]. We, therefore, evaluated whether conjugation of antigenic peptides to the higher affinity anti-MHC class II VHH DC15 would be capable of eliciting CD8T cell priming.

Here, we evaluate a novel strategy of using MHC class II expression to target CD8T cell epitopes to professional APCs. We further evaluate the combination with Neo-2/15 and show augmentation of CD8T cell responses in a preclinical model of melanoma.

2. Results

We expressed the high-affinity anti-MHC class II VHH clone DC15 or a control VHH clone 96G3 m (VHHcont) with an LPETGG sortase recognition motif at the C-terminus [22–24]. Sortase was used to install GGG-TAMRA, and the resultant fluorescently labelled DC15 was shown to bind to MHC class II positive B cells by flow cytometry, validating proper expression and folding (figure 1*a*). Antigenic peptides were synthesized with N-terminal triglycine motifs (G_3) and linked to the VHHs using recombinant 7+ sortase (figure 1*b*). Peptides also contained a biotin tag for detection of properly conjugated VHHs as determined by immunoblot with streptavidin–HRP and detection of a biotin-containing protein at 15 kDa (figure 1*c*). The concentration of properly conjugated VHH-peptide was determined by anti-biotin ELISA (figure 1*d*). Anti-biotin ELISA provides a quantitative readout of properly conjugated material, and this method was used subsequently to determine the concentration of VHH-peptide conjugates.

To determine whether conjugation to DC15 enhanced presentation of antigenic peptides on MHC class I, DC15 or VHHcont were conjugated to SIINFEKL peptide, the ovalbumin epitope recognized by CD8T cells from OT-I transgenic mice [25]. VHH-peptide conjugates or molar equivalents of free VHH admixed with SIINFEKL were pulsed onto anti-CD40-activated B-cell blasts (APCs) for 30 min. APCs were washed and cocultured with OT-I T cells. CD8T cell activation was measured by multiple parameters including proliferation, production of IFNγ and upregulation of the activation markers CD69 and CD25 (figure 2). Importantly, the amounts of peptide used in these cocultures were below that required for the activation of OT-I T cells by surface loading onto MHC class I, as evidenced by minimal activation induced by DC15 admixed with free peptide at concentrations lower than 300 pM (figure 2, blue bars).

We next assessed whether DC15-conjugated SIINFEKL could activate naive OT-I T cells *in vivo* better than peptides conjugated to an irrelevant control VHH. To this end, we injected equimolar amounts of DC15-SIIN or VHHcont-SIIN into the left foot pad of C57BL/6 mice that had received CFSE-labelled naive OT-I T cells by adoptive transfer. Contralateral footpads were injected with PBS to provide an internal negative control for each mouse. Popliteal lymph nodes were harvested 3 days later, and proliferation indexes were calculated based on CFSE dye dilution of proliferating OT-I T cells. At both 2 and 10 ng doses of vaccine, DC15 conjugation induced superior CD8T cell activation compared with VHHcont (figure 3*a*). This effect was dependent on MHC class II expression, as DC15-SIIN was less effective in mice genetically deficient in MHC class II compared with wild-type controls (figure 3*b*).

MHC class II is expressed by multiple cell types, including B cells, macrophages and dendritic cells. Of these, B cells are by far the most abundant cell type in lymph nodes, and several groups have proposed that B cells serve as an antigen sink, given their inability to prime naive CD8T cells [26–28]. CD8T cells are instead primed through interactions

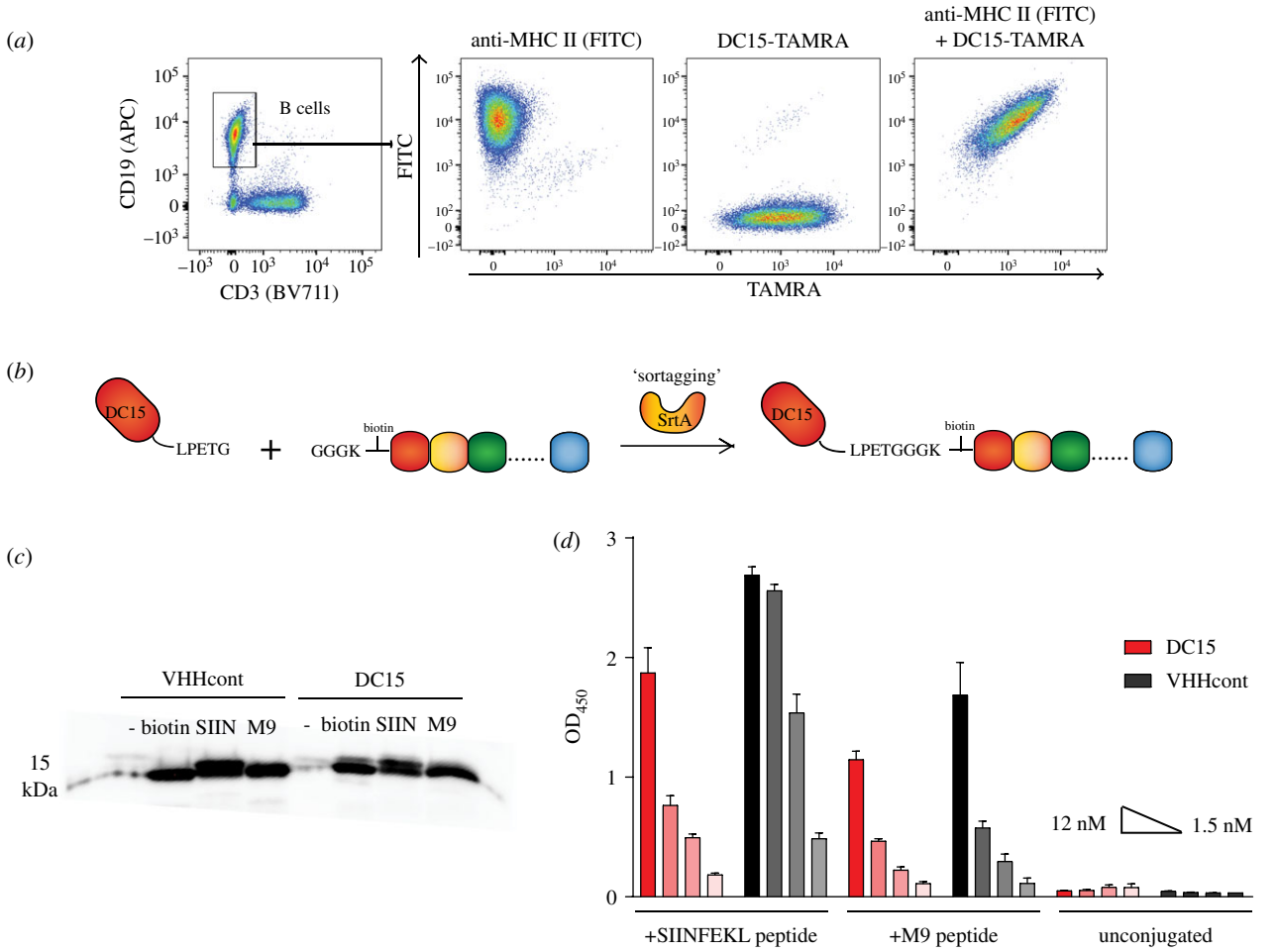

Figure 1. Construction of peptide vaccine conjugated to anti-MHC class II nanobody DC15. (*a*) Mouse spleen cells were stained with antibodies to CD3, CD19, MHC class II and DC15-TAMRA as indicated and analysed by flow cytometry. DC15-TAMRA and anti-MHC class II were used at equimolar ratios. (*b*) Scheme for production of antigen-loaded DC15. The MHC class II-specific VHH DC15 is expressed with a C-terminal LPETGG sortase recognition motif. Antigenic peptides are synthesized with an N-terminal triglycine motif for sortase-mediated conjugation to DC15. Multiple peptide epitopes may also be linked in tandem array. (*c*) VHHs and VHH conjugates were analysed by SDS–PAGE followed by transfer to nitrocellulose membrane and analysis with streptavidin–HRP. (*d*) Anti-biotin ELISA was performed on titrated samples of VHH and VHH conjugates as indicated. Peptides used were from ovalbumin (SIINFEKL) or the melanoma antigen TRP1 (M9).

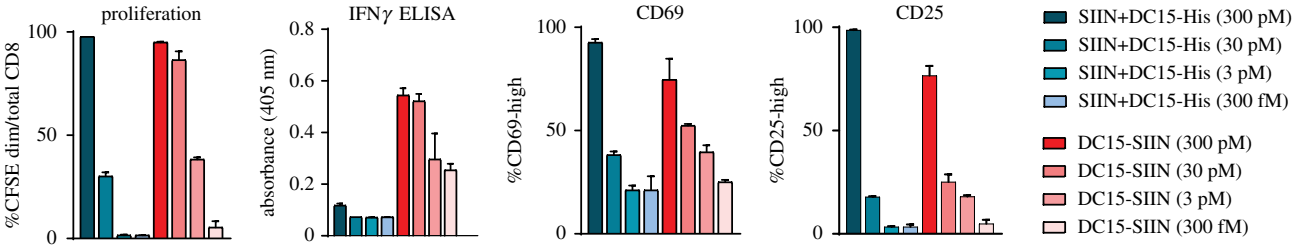

Figure 2. DC15 targeting increases antigen-presentation *in vitro*. B cells were isolated from mouse spleen by negative selection using CD43 magnetic beads and cultured with agonistic anti-CD40 for 3 days to induce B-cell blasts for use as APCs. APCs were pulsed for 30 min with the indicated concentrations of DC15 either admixed with (blue bars) or directly conjugated to SIINFEKL peptide (red bars). APCs were then washed to remove any unbound or non-internalized antigen and cocultured with CFSE-labelled OT-I T cells. Proliferation was measured by flow cytometry after 72 h. IFNγ was measured by ELISA of 72 h culture supernatants. CD69 and CD25 were measured by flow cytometry at 24 h from replicate cultures. Representative of three independent experiments. Error bars are s.e.m.

with dendritic cells, with Batf3+ CD103+ cross-presenting cells showing superior T-cell priming compared with other DC subsets [29]. To determine whether DC15-SIIN targeting is affected by the presence of a B-cell sink, we vaccinated μMT−/− mice that lack peripheral B cells [30]. DC15-SIIN vaccination elicited similar OT-I T-cell responses in both wild-type and μMT−/− mice (figure 3*c*), suggesting that MHC class II+ dendritic cells are more likely the relevant APC in this setting. We confirmed that cross-presentation of SIINFEKL peptide on MHC class I is required, as vaccination responses failed to be elicited in β2m−/− mice lacking expression of MHC class I (figure 3*c*). Collectively, these experiments demonstrate that targeting of antigenic peptide to MHC class II+ cells *in vivo* elicits CD8T cell priming, likely through the conventional pathway of cross-presentation on MHC class I by specialized dendritic cells.

DC15 can be easily conjugated to a variety of peptides, and we hypothesized that this platform could be used for neoantigen vaccines in cancer. To test this, we used a pancreatic cancer cell line KPC.1 derived from a spontaneously arising tumour from a *LSL-Kras*^{G12D}*;p53+/flox,p48-cre* mouse [31]. The donor mouse was 95% C57BL/6 background and matched for MHC haplotype. However, 5% of non-C57BL/

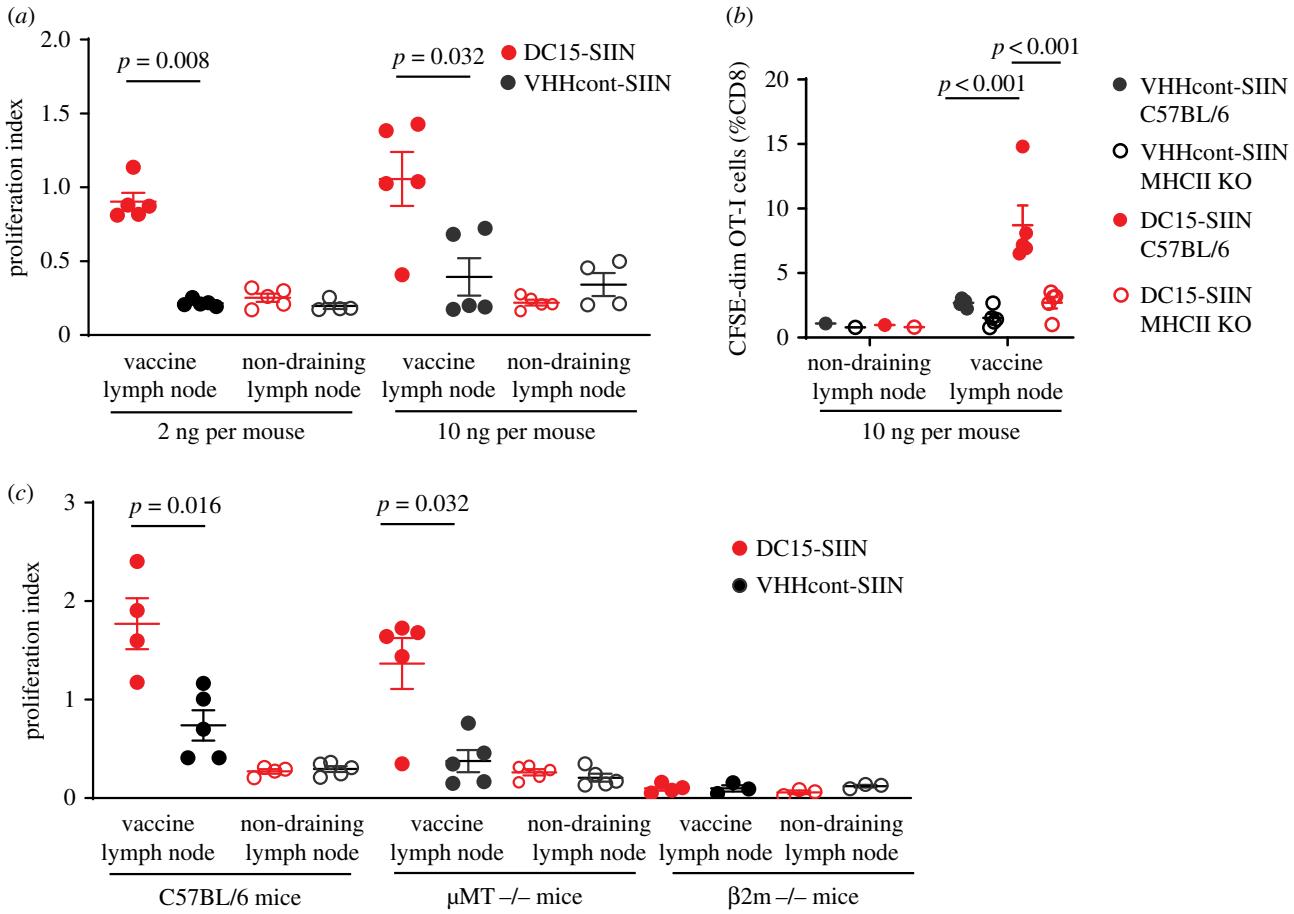

Figure 3. DC15 targeting increases CD8T cell priming *in vivo* at low doses and does not require B cells. Pooled spleen and lymph node cells from OT-I mice were labelled with CFSE and transferred intravenously into C57BL/6 recipients at 10^6 cells per mouse. (*a*) Mice were then immunized in the left footpad with DC15-SIIN or VHHcont-SIIN at 2 or 10 ng per mouse. Right footpads were injected with PBS. Popliteal lymph node cells were collected 72 h later and analysed by flow cytometry. Proliferation index was calculated as the ratio of mitotic events : progenitor cells. Representative of four independent experiments. (*b*) OT-I cells were transferred into C57BL/6 or MHC class II-deficient hosts. Host mice were immunized with 10 ng per mouse DC15-SIIN or VHHcont-SIIN. Proliferation was measured as the per cent of CFSE-dim Vα2+ Vβ5+ OT-I cells out of total CD8+. (*c*) OT-I cells were transferred into C57BL/6, μMT−/− or β2m−/− hosts. Host mice were immunized with 10 ng per mouse DC15-SIIN or VHHcont-SIIN. Proliferation indexes were calculated as in (*a*). Representative of two independent experiments.

Table 1. Model neoantigens from KPC.1 cells used in this study.

	MHC I	gene	epitope sequence	netMHC score	mRNA expression (FPKM)
Neo1	H-2-Db	Lars	NMIEAGDAL	1.5	6943
Neo2	H-2-Kb	Hjurp	VSALSSRV	1.75	3608
Neo3	H-2-Db	Smcr8	RALRKQQPI	0.2	1838
Neo4	H-2-Db	Smcr8	VSIPPQSYI	1.3	1838
Neo5	H-2-Kb	Kntc1	TGLRFHEL	0.24	1712
Neo6	H-2-Kb	Cdt1	MSYRFRQE	0.17	1711
Neo7	H-2-Db	Cdt1	GQIKTVYPM	0.9	1711
Neo8	H-2-Db	Cdt1	EMFHSMDTI	2	1711
Neo9	H-2-Db	Slc9a1	PSLLMVVAL	1.9	954
Neo10	H-2-Kb	Gadd45gip1	SGVLPASL	1.7	938
Neo11	H-2-Kb	Ppp1r21r	KLRTYVTL	1.7	745

6 contributes to approximately 1000 SNPs. We used IEDB to identify putative MHC class I binding epitopes and used these as model neoantigens. Putative model neoantigens were ranked based on the likelihood of binding to MHC class I (K^b or D^b) and their relative expression level in cultured KPC.1 cells by RNAseq analysis (table 1). The top 11 model neoantigens were synthesized with triglycine motifs and biotin at the N-termini, and sortase was used to conjugate them to DC15 or VHHcont (figure 4*a*). Two peptides (neo8 and neo9) had poor solubility and were not analysed further. The remaining VHH-peptides were pooled and used to vaccinate C57BL/6 mice at days 14 and 7 prior to inoculation with subcutaneous KPC.1 cells. Unfortunately, no differences were observed between the rate of growth or

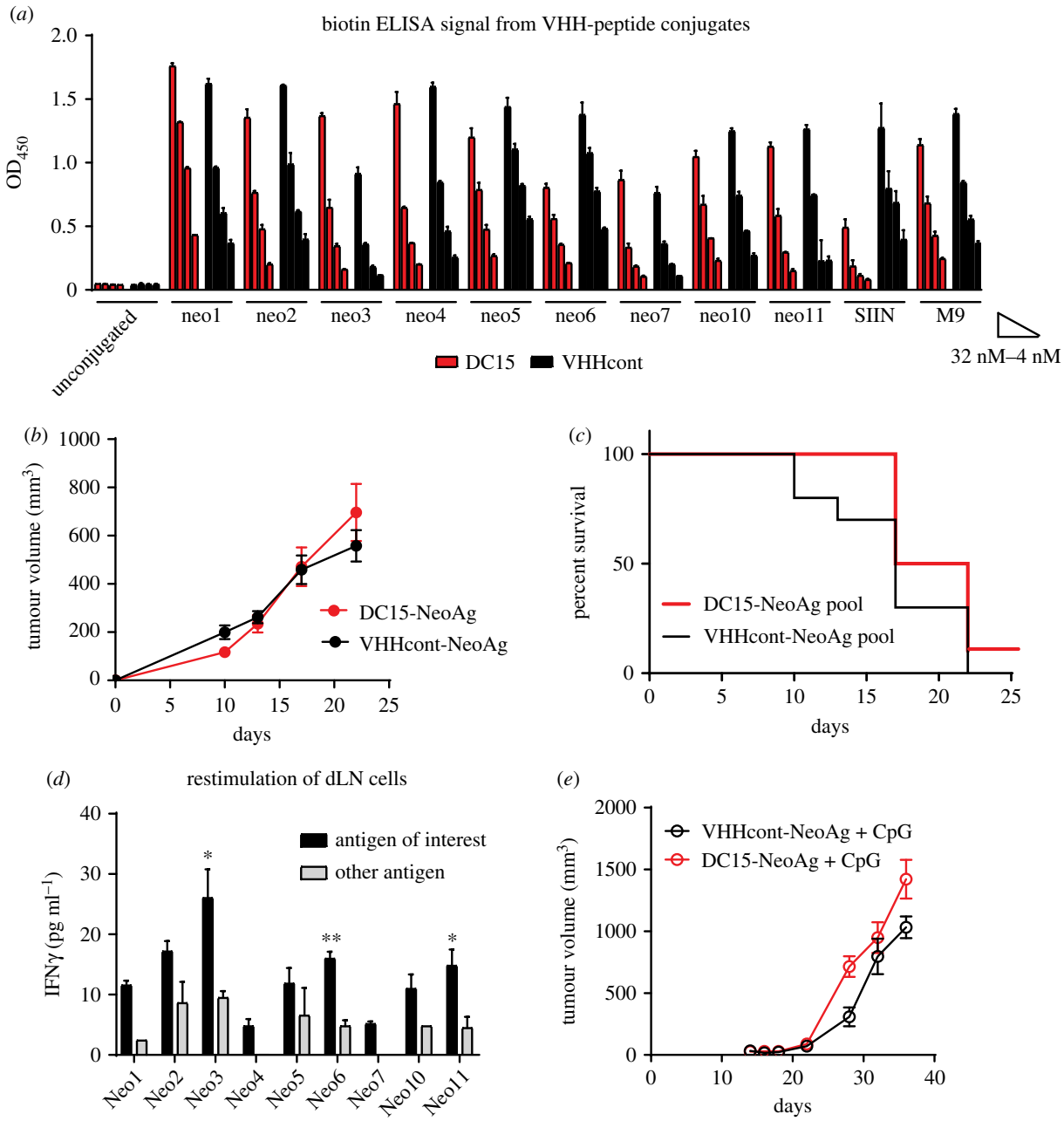

Figure 4. DC15-based neoantigen vaccine in pancreatic cancer is ineffective at inducing T-cell responses. (*a*) Neoantigens from table 1 were synthesized as biotinylated 18-mer peptides containing the 8 or 9-mer neoantigen with three or four flanking residues from the original gene and GGG motifs at their N-termini. Peptides were conjugated to DC15 or VHHcont using sortase. Conjugation was validated by anti-biotin ELISA. (*b*) All nine neoantigens were pooled at 2 ng per VHH-neo construct per mouse per immunization (18 ng total protein per injected paw). Mice were immunized in both hind footpads at Days 14 and 7 prior to inoculation of 250 000 KPC.1 cells subcutaneously. Tumour growth was monitored over time. $N = 10$ mice per group. (*c*) Survival of mice shown in (*b*). (*d*) C57BL/6 mice were vaccinated as in (*b*). Draining popliteal LNs were harvested 7 days after the second immunization, and dissociated cells were cultured with 1 ng ml^{-1} of the indicated neoantigen peptides or irrelevant SIINFEKL control. IFNγ was measured by ELISA of 48 h culture supernatants. *$p < 0.02$, **$p < 0.001$. Error bars are s.e.m. of biological duplicates. (*e*) Mice were vaccinated as in (*b*) except that 15 ng CpG was admixed with the VHH conjugates prior to inoculation. Mice were challenged with 250 000 KPC.1 cells subcutaneously. Tumour growth was monitored over time. $N = 5$ mice per group.

overall survival of tumour-bearing mice (figure 4*b*,*c*). To determine whether DC15-NeoAg pool induced antigen-specific T cells, a cohort of non-tumour-bearing C57BL/6 mice were vaccinated at days 14 and 7 prior to harvest of vaccine draining LN cells and restimulation *ex vivo* with each model neoantigen (figure 4*d*). Although most of the peptides induced greater IFNγ production than their irrelevant controls, the overall levels of IFNγ production were low, consistent with lack of a vigorous neoantigen-specific T-cell response. We hypothesized that the addition of the TLR9 ligand CpG would adjuvant the DC15-NeoAg response; however, even with the addition of CpG, tumours grew progressively in both VHHcont-NeoAg and DC15-NeoAg vaccinated mice (figure 4*e*).

Pancreatic cancer is notoriously refractory to CD8T cell-based therapies [32]. To test the effects of DC15-peptide vaccination in a more amenable setting, we used the B16 melanoma model. Tyrosinase-related protein 1 (TRP1) is a CD8T cell antigen in both mice and humans, and TRP1-specific CD8T cells can be tracked using specific tetramers [33]. We conjugated DC15 or VHHcont to the TRP1 peptide M9 (TAPDNLGYM), which has an alanine to methionine substitution in the ninth position anchor residue to enhance the stability of the H-2D^{b} peptide complex [33,34]. C57BL/6

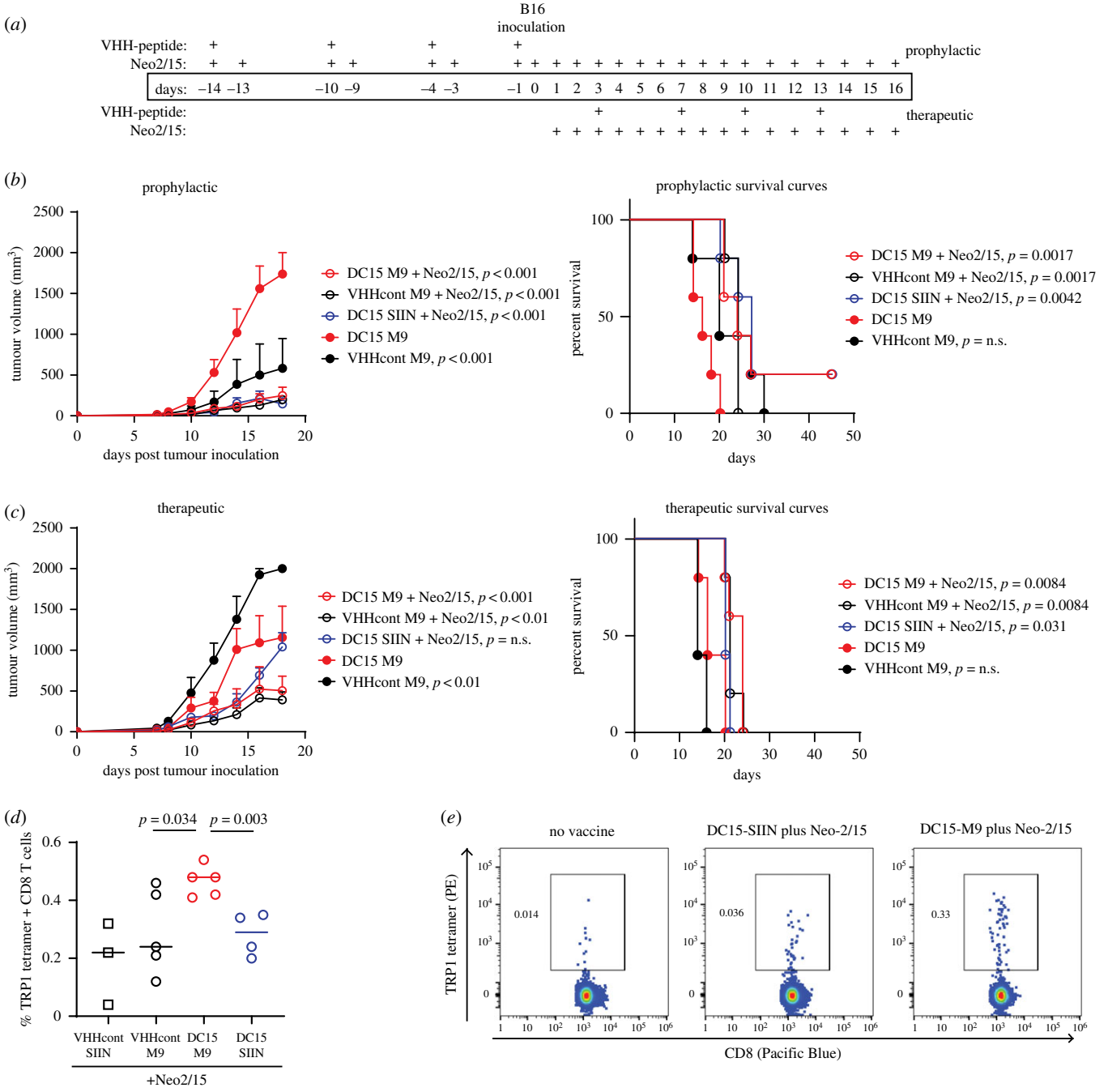

Figure 5. Combination of DC15-based vaccination and Neo2/15 leads to anti-tumour immunity in the B16 melanoma model. (*a*) Schedule of treatments for prophylactic and therapeutic experimental cohorts. Neo2/15 was used at 10 µg per dose; VHH-peptides were used at 10 ng per dose. M9 peptide was used as the relevant antigenic epitope; SIINFEKL was included as a negative control. $N = 5$ mice per group. Experiments were conducted in parallel such that all mice were inoculated subcutaneously with 250 000 B16 cells on the same day. (*b*) Tumour growth and survival of mice in the prophylactic cohorts. *p*-values shown are comparisons with the DC15-M9 vaccinated group. (*c*) Tumour growth and survival of mice in the therapeutic cohorts. *p*-values shown are comparisons with the DC15-M9 vaccinated group. (*d*) C57BL/6 mice were vaccinated with 10 ng per dose of VHH-peptide on Days 0 and 4. Mice received 10 µg per mouse Neo2/15 daily starting on Day 0. Draining lymph nodes were harvested on Day 9, stained and analysed by flow cytometry. (*e*) C57BL/6 mice were inoculated with B16 tumours and left untreated. When tumours reached greater than 1 cm^3, draining lymph node cells were harvested from mice with progressively growing tumours as well as from the single surviving mice in the DC15-SIIN/Neo2/15 and DC15-M9/Neo2/5 prophylactic cohorts shown in (*b*). Cells were stained with anti-CD8 and TRP1 tetramers. Flow cytometry plots are gated on total CD8+ cells.

mice were vaccinated with 10 ng per dose of DC15-M9, VHHcont-M9 or DC15-SIIN (used here as an irrelevant control peptide) according to the schedule shown in figure 5*a*. Two experiments were performed simultaneously, one in which mice were vaccinated prior to tumour challenge (prophylactic) and one in which mice were vaccinated starting 3 days after tumour challenge (therapeutic). Given the poor adjuvant effects observed with CpG (figure 4*e*), we decided to use the synthetic IL-2 mimetic Neo2/15 instead. Both IL-2 and Neo2/15 were previously shown to have modest single-agent activity and to augment responses to TA99, a TRP1-specific antibody, in the B16 model [17,35].

We observed a significant decrease in tumour growth in all cohorts that received Neo2/15, consistent with the known single-agent activity of this compound (figure 5*b*,*c*). All mice were inoculated with B16 tumours on the same

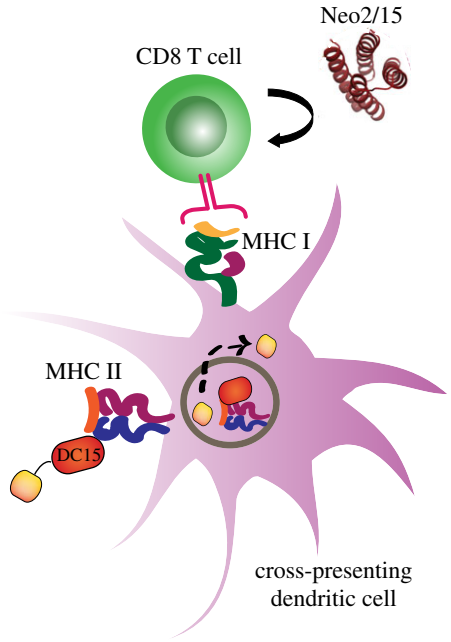

Figure 6. Diagram of tumour vaccine platform. DC15 binds to MHC class II on the surface of dendritic cells, which is internalized into endolysosomes, allowing for the proteolytic release of the antigenic peptide cargo (yellow). The antigenic peptide is then crosspresented on MHC class I to CD8T cells. Neo2/15 supports the proliferation and survival of newly primed CD8T cells.

day, allowing for comparison across all cohorts. Intriguingly, the tumour growth delay induced by Neo2/15 was more pronounced in the prophylactic setting, suggesting that tonic low-level T-cell activation at the time of tumour implantation may provide some protective benefit. We did not observe a significant difference in tumour control or survival between mice that received DC15-M9 versus VHHcont-M9, and indeed, the DC15-M9 prophylactic cohort showed increased tumour growth compared with VHHcont-M9. We speculate that this could be due to DC15 binding to B cells expressing MHC class II. However, in the therapeutic cohort, DC15-M9 vaccination performed better than VHHcont-M9. Inoculation of the tumour itself acts as a complex mixture of vaccine antigens and it could be that priming with a single peptide followed by boosting with a complex mixture is less effective than priming with a complex mixture and boosting with a single peptide [36].

To ascertain whether DC15-M9 vaccination induced any TRP1-specific CD8T cells, we first evaluated mice treated according to the prophylactic schedule shown in figure 5*a*, but harvested at Day 5. These mice received two doses of vaccine and Neo2/15 but were not challenged with the tumour. At this early time point, we observed that DC15-M9 vaccinated mice had TRP1 tetramer+ CD8T cells at a frequency above the baseline level seen in mice vaccinated with SIINFEKL irrelevant peptide (figure 5*d*). To determine whether vaccine-elicited CD8T cells were observed in mice that had survived tumour challenge, we harvested draining lymph nodes from the two surviving tumour-free mice, one that had received DC15-SIIN/Neo2/15 and one that had received DC15-M9/Neo2/15. TRP1 tetramer staining showed a 10-fold increase in TRP1-specific CD8T cells in the mouse that had received DC15-M9 vaccination compared with the mouse that had received DC15-SIIN (figure 5*e*). These results suggested that while Neo2/15 is capable of augmenting a polyclonal endogenous response to B16 tumours, that in DC15-M9 vaccinated mice, the vaccine-elicited CD8T cells may also contribute to tumour control (figure 6).

3. Discussion

Cancer vaccines have been fraught with challenges, and the field is only now beginning to see successful phase I trials after nearly three decades of effort [37,38]. A successful vaccine must incorporate three parts: high-quality antigens, potent adjuvants and a robust delivery platform. Here, we present a novel approach, namely, using a high-affinity MHC class II-specific VHH to target antigenic peptides to antigen-presenting cells. This strategy was effective using as little as 2 ng of protein conjugate to elicit CD8T cell responses *in vivo* to the model antigen SIINFEKL. Other antigens could be easily conjugated through the sortase handle installed on the VHH, enabling us to rapidly evaluate a panel of neoantigen candidates in a pancreatic cancer model. Although none of these candidates afforded tumour protection, the ease of the delivery platform allowed us to test and eliminate nonproductive candidates quickly. Tandem addition of peptide epitopes is also trivial, either through direct genetic linkage or through repeat sortagging of individual subunits. Although DC15 is specific for mouse MHC class II, a human-specific version that recognizes multiple HLA-DR haplotypes has been reported [39].

Alpaca-derived VHHs have shown utility in preclinical models of cancer diagnostics and therapy [21]. In addition to MHC class II, other endocytosed receptors have been targeted, and CD11b-specific VHHs are capable of generating CD8T cell responses [40]. VHHs have also been used to deliver immunomodulatory cytokines to the tumour microenvironment [41], and as immune-positron emission imaging reagents for cancer and targets of cancer therapies [40,42–45]. Due to their unusually stable folding, single-domain VHHs generate stable CAR-T constructs and can be used to target solid tumours in mice [46]. Delivery of increasingly complex vaccine cargo is a reasonable next step, perhaps aided by the selection of VHHs specific for targets more exclusively restricted to cross-presenting dendritic cells. MHC class II targeted VHHs have been used as vaccines for both infectious disease and cancer in settings where CD4T cell responses and antibody responses conferred protective immunity [19,20]. They have thus far been less good at eliciting CD8T cell responses, although we have now demonstrated proof-of-principle efficacy using the high-affinity anti-MHC class II targeted VHH clone DC15.

We chose to support newly primed CD8T cell responses using the synthetic IL-2 mimetic Neo2/15. This highly stable protein is incapable of binding to IL2Ra (CD25), giving it a favourable safety profile [17]. Importantly, Treg induction is less pronounced than with regular IL-2, and a direct comparison of Neo2/15 with equimolar recombinant IL-2 showed greater anti-tumour activity of the synthetic cytokine [31]. Here, we also observed significant activity of Neo2/15 even when combined with DC15 conjugated to an irrelevant peptide. These results highlight the importance of a polyclonal response to achieving successful tumour control [47]. Neo2/15 was also able to support vaccine-elicited CD8T cells, as evidenced by increased TRP1 tetramer+ cells early in the vaccination protocol and in the surviving mouse that had

received DC15-M9 vaccination. We are moderately encouraged that the DC15 platform can be used to prime CD8T cell responses in the setting of cancer.

4. Material and methods

4.1. Mice

All animal protocols were approved by the Dana-Farber Cancer Institute Committee on Animal Care (protocol nos 14-019 and 14-037) and are in compliance with the NIH/NCI ethical guidelines for tumour-bearing animals. The following mouse strains were purchased from Jackson Labs: C57BL/6 (000664), μMT$^{-/-}$ (002249), β2m$^{-/-}$ (002087), OT-I (003831) and I-Ab$^{-/-}$ (005589).

4.2. Subcutaneous tumour inoculations

The B16F10 cell line was purchased from ATCC and used within 1 year of receipt. The KPC.1 cells were a gift from A. Maitra (MD Anderson Cancer Center). Cells were cultured in complete RPMI media and were verified by Charles River Laboratories to be mouse pathogen free and mycoplasma free less than six months prior to use. Cells were grown to 80% confluency, dissociated using 0.25% trypsin, washed twice in PBS and suspended in fresh sterile PBS for inoculation into mice. Mice were inoculated with 250 000 tumour cells in 150 µl total volume. Tumour size was monitored by precision calipers every 2–3 days. Mice were euthanized when tumour size reached 2 cm^3, ulcerated or showed signs of morbidity consistent with the NIH/NCI ethical guidelines for tumour-bearing animals.

4.3. OT-I cell transfer and footpad vaccinations

Spleen and lymph nodes cells were isolated from 2–3 donor OT-I mice, subjected to hypotonic lysis to remove erythrocytes, and labelled with CFSE (Invitrogen, C34554) according to the manufacturer's protocol. CFSE-labelled cells were washed twice in PBS, counted and suspended at 1 million cells per 150 µl sterile PBS. Cells were then transferred by tail vein injection into host mice (1 million cells per mouse). Within 24 h, host mice were vaccinated by intradermal injection of 30 µl sterile PBS or VHH conjugates with or without CpG (Invivogen, tlrl-1826, 20 µg mouse^{-1}) into the hind footpads. Three days later, mice were euthanized by CO_2 inhalation and popliteal lymph nodes were harvested. Lymph node cells were stained with anti-CD8 and TRP1 tetramer (NIH tetramer core facility) and analysed by flow cytometry using a Sony SP6800 spectral flow cytometry. CFSE-dim cells were gated by the number of cell divisions and the proliferation indexes were calculated.

4.4. Cell culturing

Primary cells and cell lines were cultured in RPMI 1640 medium (Gibco, 11875119) supplemented with 10% heat-inactivated FBS (Omega Scientific catalogue no. FB-11), 2 mM L-glutamine (Gibco), 100 U ml^{-1} penicillin-streptomycin (Gibco), 1 mM sodium pyruvate (Gibco), 0.1 mM nonessential amino acids (Gibco) and 0.1 mM β-mercaptoethanol (Sigma). B cells were isolated from C57BL/6 mouse spleen and lymph nodes using magnetic bead enrichment (Thermo Fisher Dynabeads Mouse CD43, catalogue no. 11422D) and stimulated with agonistic anti-CD40 (clone HM40-3, 2 µg ml^{-1} BD Cell Analysis catalogue no. 553721). For cytokine analysis, CD40-activated B cells and CD8$^+$ T cells were cocultured at a 1 : 1 ratio, and supernatants were harvested after 72 h. IFNγ was quantified by ELISA (Biolegend catalogue no. 430806). Supernatants were diluted 1 : 4 prior to analysis and used at 100 µL volume per well of a 96-well plate. For culturing of lymph node cells from vaccinated mice in figure 4, culture supernatants were not diluted prior to ELISA.

4.5. Flow cytometry

Cells were incubated with antibody staining mix including 2% fetal calf serum for 30 min at 4°C, washed once in PBS and resuspended in 1% formalin in PBS. The analysis was performed on a Sony SP6800 spectral flow cytometer. Data were analysed using FloJo software. Cells were first gated on CD45$^+$ cells using SSClow as a proxy for viability. Flow cytometry antibodies used in this study were purchased from Biolegend (CD8 (clone 53-6.7), CD25 (clone 3C7) and CD69 (clone H1.2F3)). TRP1 H-2D^b tetramer was provided by the NIH Tetramer Core Facility. Tetramer staining was performed at room temperature for 30 min.

4.6. Expression and purification of sortase A

BL21 (DE3) cells were transformed with pET30b+ containing 7+ SrtA construct [23] and cultured at 37°C overnight in 5 ml of Luria Broth media supplemented 34 µg ml^{-1} kanamycin. This was then was used to inoculate 200 ml of terrific broth (TB) media supplemented with 34 µg ml^{-1} kanamycin (Sigma K4000) and cultured at 37°C until and OD600 approximately 0.6, at which point 1 mM isopropylthio-β-galactopyranoside (IPTG, Teknova T0918) was added and cultures induced overnight at 30°C. Cells were harvested by centrifugation (6000 rpm, 30 min, 4°C) and the resulting pellet was resuspended in 50 ml of wash buffer (50 mM Tris, 150 mM NaCl, 10 mM imidazole, pH 7.6) and lysed by sonication. To harvest the soluble fraction, the lysate was again centrifuged (6000 rpm, 30 min, 4°C) and the resulting supernatant was incubated with 2 ml of Ni-NTA agarose resin (Qiagen, 30230) on a rotating wheel at 4°C overnight. The resin was washed three times with 10 ml of wash buffer in a disposable gravity column. After the addition of 5 ml of elution buffer (50 mM Tris, 150 mM NaCl, 500 mM imidazole, pH 7.6), the eluent was buffer exchanged in 3 kDa MWCO ultrafiltration device (Millipore) and into 50 mM Tris (pH 7.5) and concentrated to 200 µl. Expression and purification of the protein were confirmed by SDS–PAGE analysis using 4–20% polyacrylamide gel (Bio-Rad). The concentration of the protein was calculated using A280 absorbance on a NanoDrop (Thermo).

4.7. Expression and purification of VHHs

WK6 cells were transformed with pHEN6-DC15 or VHHcont and cultured at 37°C overnight in 50 ml of TB (Sigma T0918) supplemented with 100 µg ml^{-1} ampicillin (Sigma A0166) at 225 rpm. This was then used to inoculate 1 l of TB supplemented with 100 µg ml^{-1} ampicillin and cultured at 37°C until OD600 approximately 0.6, at which point 1 mM IPTG (Teknova, I3325) was added and cultures induced overnight at 30°C. Cells were harvested by centrifugation (1370g, 15 min, 4°C). The periplasmic fraction was then released via osmotic shock by incubating the pellet in 30 ml of 1× TES

buffer (0.2 M Tris, 0.65 mM EDTA, 0.5 M sucrose) on a rotating wheel at 4°C for 1 h, and then diluted with an additional 30 ml of 0.25× TES buffer, and rotated overnight at 4°C. After centrifugation (9700*g*, 15 min, 4°C), the supernatant was incubated with 2 ml of Ni^{2+} NTA agarose resin (Qiagen, 30230) on a rotating wheel at 4°C for 1 h. The resins were pelleted at 325*g* and the supernatant was collected as 'flow-through'. The resins were washed two times with 50 ml of wash buffer (50 mM Tris, pH 8, 150 mM NaCl, 10 mM imidazole) via centrifugation at 325*g*. The resins were transferred to disposable gravity-flow columns (Life Technologies, 29924) and eluted 2×with 4 ml elution buffer (50 mM Tris, 150 mM NaCl, 500 mM imidazole, pH 7.6). The eluent was buffer exchanged using 30 k MWCO ultrafiltration devices (Millipore) and into LPS-free PBS and concentrated via 10 k MWCO ultrafiltration devices (Millipore). Proteins were tested for endotoxin using a Pierce LAL chromogenic endotoxin quantitation kit (Thermo, 88282), and confirmed to be under 0.2 EU mg ml^{-1}. Expression and purification of the protein were confirmed by SDS–PAGE analysis using 12% polyacrylamide gel (Bio-Rad), and the concentration of the protein was measured by BCA assay (Thermo Scientific, 23235).

4.8. VHH conjugation using SrtA

Biotinylated peptides were synthesized by the MIT Koch Institute Biopolymers Facility. 2.5 µM SrtA and 1 mg VHH-LPETGG were added to a 5× molar excess GGG-peptide or GGG-TAMRA in 50 mM Tris and 150 mM NaCl with 10 mM $CaCl_2$. The total reaction volume was 1.7 ml. The resulting mixture was incubated at 4°C for 120 min. Unconjugated VHH was removed via Ni NTA^{2+} agarose (Qiagen) incubation at 4°C for 10 min. The supernatant was collected as conjugated VHH-peptide. Conjugation efficiency was determined either by SDS–PAGE analysis and immunoblotting with streptavidin–HRP or by anti-biotin ELISA.

4.9. SDS–PAGE analysis and streptavidin blotting

A 15% SDS–PAGE gel was cast using National Diagnostics ProtoGel reagents (ProtoGel 30% EC-890, 4X Resolving buffer EC-892, Stacking buffer EC-893, Running buffer EC-870). 0.5 µg VHH-peptide was dyed (3X Laemmli loading dye, 1 M Tris pH 6.8, 20% SDS, glycerol, β-mercaptoethanol, bromophenol blue) and loaded on the gel and then run at 150 V until the dye front reached the bottom of the gel. The Bio-Rad Trans-Blot Turbo system (17001917) was used for the transfer of the gel to a PVDF membrane. Streptavidin–HRP (Biolegend, 405210) diluted 1 : 10 000 in 3% BSA in TBST was used for detection of biotin signal. Chemiluminescence reagent (Perkin-Elmer, NEL103E001EA) was added prior to imaging on a Bio-Rad Chem-iDoc imaging system.

4.10. Anti-biotin ELISA

96-well high-affinity plates (Corning, 9018) were coated with VHH-peptide in coating buffer ((3.03 g Na_2CO_3, 6 g $NaHCO_3$) l^{-1}, pH 9.6). Plates were left at 4°C overnight. The next day, plates were washed 3× PBST, then blocked 1 h at room temperature with PBS + 10% FBS (blocking buffer). Plates were washed 3× again with PBST, then 1 : 1000 Avidin–HRP (Biolegend, 405103) in blocking buffer was added for 1 h. Plates were washed 5× with TBST, then developed with 100 µl TMB (Sigma, T8665). The reaction was stopped using 1 M HCl (Sigma, 258148), then read on a plate reader at absorbance 540 nm.

4.11. Neoantigen prediction

Neoantigen candidates were obtained by analysing SNPs found in the KPC.1 cell line via RNA sequencing. Briefly, RNA from three samples of the KPC cell line was sequenced and aligned to the mm10 genome using STAR. SNPs were called using the Broad Institute pipeline 'RNAseq short variant per-sample calling'. Only SNPs that were common to all three samples were considered. The effect of each SNP on the protein product was predicted using the tool SnpEff [48], and the resulting mutated peptide sequence was identified by overlaying on the UP000000589 mouse proteome. Candidate binding affinity to mouse MHCI was predicted using the Immune Epitope Database (IEDB) recommended 2.22 prediction method, which uses the Consensus analysis tool to combine predictions from ANN, SMM and Comblib. Neoantigen candidates were analysed as 8-mers for H-2 K^b and 9-mers for H-2D^b with 7 and 8 amino acids flanking each side of the SNP, respectively. The top 2% of predicted binders were selected, producing a list of 48 potential neoantigens. The binding affinity of these candidates was then compared with the binding affinity of their corresponding wild-type sequence. Neoantigen candidates were then sorted in order from the largest mean expression to the smallest. The top 11 neoantigens with the largest mean expression values which also bound better to MHCI than their wild-type peptide sequence were selected for conjugation to DC15.

4.12. Statistical analysis

All tumour weight and tumour infiltrates data are presented as mean with s.e.m. error bars unless otherwise noted. Significance was determined using a two-sided Mann–Whitney test to compare ranks, without assuming Gaussian distribution. For tumour growth and survival curves, significance was determined using two-way ANOVA and a log rank Mantel–Cox test, respectively. Graphpad Prism software was used to analyse data.

Ethics. All animal protocols were approved by the Dana-Farber Cancer Institute Committee on Animal Care (protocol nos14-019 and 14-037) and are in compliance with the NIH/NCI ethical guidelines for tumour-bearing animals.

Data accessibility. All data are provided in the figures and tables.

Authors' contributions. S.J.C., P.T.B., M.A.B., A.M.-G., M.J.W., K.Z. and H.-J.J. performed experiments and analysed data. P.T.B., K.Z. and L.R.A. performed computational analysis of neoantigens. J.R.I. designed the VHH-peptide conjugation strategy and provided key insights. D.M.K. and H.L.P. supervised some experiments. M.D. and S.K.D. analysed data and supervised the study. S.K.D. wrote the manuscript with input from all of the authors.

Competing interests. We declare we have no competing interests.

Funding. This work was funded by a DOD Career Development award (no. CA150378) to S.K.D., a Claudia Adams Barr Award to J.R.I. and NIH (grant no. P01 AI098681) to D.M.K.

Acknowledgements. We thank D. A. Silva and D. Baker for providing the Neo2/15. We thank the NIH Tetramer Core Facility for provision of TRP1 tetramers.

References

1. Dougan M, Dranoff G, Dougan SK. 2019 Cancer immunotherapy: beyond checkpoint blockade. *Annu. Rev. Cancer Biol.* **1**, 55–75. (doi:10.1146/annurev-cancerbio-030518-055552)
2. Hacohen N, Fritsch EF, Carter TA, Lander ES, Wu CJ. 2013 Getting personal with neoantigen-based therapeutic cancer vaccines. *Cancer Immunol. Res.* **1**, 11–15. (doi:10.1158/2326-6066.CIR-13-0022)
3. Van Allen EM *et al.* 2015 Genomic correlates of response to CTLA-4 blockade in metastatic melanoma. *Science* **350**, 207–211. (doi:10.1126/science.aad0095)
4. Bezu L, Kepp O, Cerrato G, Pol J, Fucikova J, Spisek R, Zitvogel L, Kroemer G, Galluzzi L. 2018 Trial watch: peptide-based vaccines in anticancer therapy. *Oncoimmunology* **7**, e1511506. (doi:10.1080/2162402X.2018.1511506)
5. Ott PA *et al.* 2017 An immunogenic personal neoantigen vaccine for patients with melanoma. *Nature* **547**, 217–221. (doi:10.1038/nature22991)
6. Keskin DB *et al.* 2019 Neoantigen vaccine generates intratumoral T cell responses in phase Ib glioblastoma trial. *Nature* **565**, 234–239. (doi:10.1038/s41586-018-0792-9)
7. Hilf N *et al.* 2019 Actively personalized vaccination trial for newly diagnosed glioblastoma. *Nature* **565**, 240–245. (doi:10.1038/s41586-018-0810-y)
8. Sahin U *et al.* 2017 Personalized RNA mutanome vaccines mobilize poly-specific therapeutic immunity against cancer. *Nature* **547**, 222–226. (doi:10.1038/nature23003)
9. Hu Z, Ott PA, Wu CJ. 2018 Towards personalized, tumour-specific, therapeutic vaccines for cancer. *Nat. Rev. Immunol.* **18**, 168–182. (doi:10.1038/nri.2017.131)
10. Boyman O, Sprent J. 2012 The role of interleukin-2 during homeostasis and activation of the immune system. *Nat. Rev. Immunol.* **12**, 180–190. (doi:10.1038/nri3156)
11. Siegel JP, Puri RK. 1991 Interleukin-2 toxicity. *J. Clin. Oncol.* **9**, 694–704. (doi:10.1200/JCO.1991.9.4.694)
12. Dranoff G. 2004 Cytokines in cancer pathogenesis and cancer therapy. *Nat. Rev. Cancer* **4**, 11–22. (doi:10.1038/nrc1252)
13. Vazquez-Lombardi R *et al.* 2017 Potent antitumour activity of interleukin-2-Fc fusion proteins requires Fc-mediated depletion of regulatory T-cells. *Nat. Commun.* **8**, 15373. (doi:10.1038/ncomms15373)
14. Levin AM *et al.* 2012 Exploiting a natural conformational switch to engineer an interleukin-2 'superkine'. *Nature* **484**, 529–533. (doi:10.1038/nature10975)
15. Mott HR, Baines BS, Hall RM, Cooke RM, Driscoll PC, Weir MP, Campbell ID. 1995 The solution structure of the F42A mutant of human interleukin 2. *J. Mol. Biol.* **247**, 979–994. (doi:10.1006/jmbi.1994.0194)
16. Carmenate T, Pacios A, Enamorado M, Moreno E, Garcia-MartãNez K, Fuente D, León K. 2013 Human IL-2 mutein with higher antitumor efficacy than wild type IL-2. *J. Immunol.* **190**, 6230–6238. (doi:10.4049/jimmunol.1201895)
17. Silva DA *et al.* 2019 De novo design of potent and selective mimics of IL-2 and IL-15. *Nature* **565**, 186–191. (doi:10.1038/s41586-018-0830-7)
18. Shin JS, Ebersold M, Pypaert M, Delamarre L, Hartley A, Mellman I. 2006 Surface expression of MHC class II in dendritic cells is controlled by regulated ubiquitination. *Nature* **444**, 115–118. (doi:10.1038/nature05261)
19. Duarte JN *et al.* 2016 Generation of immunity against pathogens via single-domain antibody-antigen constructs. *J. Immunol.* **197**, 4838–4847. (doi:10.4049/jimmunol.1600692)
20. Fang T, Van Elssen CHMJ, Duarte JN, Guzman JS, Chahal JS, Ling J, Ploegh HL. 2017 Targeted antigen delivery by an anti-class II MHC VHH elicits focused alphaMUC1(Tn) immunity. *Chem. Sci.* **8**, 5591–5597. (doi:10.1039/C7SC00446J)
21. Ingram JR, Schmidt FI, Ploegh HL. 2018 Exploiting nanobodies' singular traits. *Annu. Rev. Immunol.* **36**, 695–715. (doi:10.1146/annurev-immunol-042617-053327)
22. Rashidian M *et al.* 2015 The use of (18)F-2-fluorodeoxyglucose (FDG) to label antibody fragments for immuno-PET of pancreatic cancer. *ACS Cent. Sci.* **1**, 142–147. (doi:10.1021/acscentsci.5b00121)
23. Jeong HJ, Abhiraman GC, Story CM, Ingram JR, Dougan SK. 2017 Generation of Ca^{2+}-independent sortase A mutants with enhanced activity for protein and cell surface labeling. *PLoS ONE* **12**, e0189068. (doi:10.1371/journal.pone.0189068)
24. Pishesha N, Ingram JR, Ploegh HL. 2018 Sortase A: a model for transpeptidation and its biological applications. *Annu. Rev. Cell Dev. Biol.* **34**, 163–188. (doi:10.1146/annurev-cellbio-100617-062527)
25. Hogquist KA, Jameson SC, Heath WR, Howard JL, Bevan MJ, Carbone FR. 1994 T cell receptor antagonist peptides induce positive selection. *Cell* **76**, 17–27. (doi:10.1016/0092-8674(94)90169-4)
26. Bijker MS, Van Den Eeden SJF, Franken KL, Melief CJM, Offringa R, Van Der Burg SH. 2007 CD8+ CTL priming by exact peptide epitopes in incomplete Freund's adjuvant induces a vanishing CTL response, whereas long peptides induce sustained CTL reactivity. *J. Immunol.* **179**, 5033–5040. (doi:10.4049/jimmunol.179.8.5033)
27. Welters MJ *et al.* 2008 Induction of tumor-specific CD4+ and CD8+ T-cell immunity in cervical cancer patients by a human papillomavirus type 16 E6 and E7 long peptides vaccine. *Clin. Cancer Res.* **14**, 178–187. (doi:10.1158/1078-0432.CCR-07-1880)
28. Kenter GG *et al.* 2008 Phase I immunotherapeutic trial with long peptides spanning the E6 and E7 sequences of high-risk human papillomavirus 16 in end-stage cervical cancer patients shows low toxicity and robust immunogenicity. *Clin. Cancer Res.* **14**, 169–177. (doi:10.1158/1078-0432.CCR-07-1881)
29. Hildner K *et al.* 2008 Batf3 deficiency reveals a critical role for CD8alpha+ dendritic cells in cytotoxic T cell immunity. *Science* **322**, 1097–1100. (doi:10.1126/science.1164206)
30. Kitamura D, Roes J, Kuhn R, Rajewsky K. 1991 A B cell-deficient mouse by targeted disruption of the membrane exon of the immunoglobulin mu chain gene. *Nature* **350**, 423–426. (doi:10.1038/350423a0)
31. Hingorani SR *et al.* 2003 Preinvasive and invasive ductal pancreatic cancer and its early detection in the mouse. *Cancer Cell.* **4**, 437–450. (doi:10.1016/S1535-6108(03)00309-X)
32. Balachandran VP, Beatty GL, Dougan SK. 2019 Broadening the impact of immunotherapy to pancreatic cancer: challenges and opportunities. *Gastroenterology* **156**, 2056–2072. (doi:10.1053/j.gastro.2018.12.038)
33. Dougan SK, Dougan M, Kim J, Turner JA, Ogata S, Cho H-I, Jaenisch R, Celis E, Ploegh HL. 2013 Transnuclear TRP1-specific CD8T cells with high or low affinity TCRs show equivalent antitumor activity. *Cancer Immunol. Res.* **1**, 99–111. (doi:10.1158/2326-6066.CIR-13-0047)
34. Clancy-Thompson E *et al.* 2018 Altered binding of tumor antigenic peptides to MHC class I affects CD8(+) T cell-effector responses. *Cancer Immunol. Res.* **6**, 1524–1536. (doi:10.1158/2326-6066.CIR-18-0348)
35. Moynihan KD *et al.* 2016 Eradication of large established tumors in mice by combination immunotherapy that engages innate and adaptive immune responses. *Nat. Med.* **22**, 1402–1410. (doi:10.1038/nm.4200)
36. Shaffer JS, Moore PL, Kardar M, Chakraborty AK. 2016 Optimal immunization cocktails can promote induction of broadly neutralizing Abs against highly mutable pathogens. *Proc. Natl Acad. Sci. USA* **113**, E7039–E7048. (doi:10.1073/pnas.1614940113)
37. Rosenberg SA, Yang JC, Restifo NP. 2004 Cancer immunotherapy: moving beyond current vaccines. *Nat. Med.* **10**, 909–915. (doi:10.1038/nm1100)
38. Ott PA, Fritsch EF, Wu CJ, Dranoff G. 2014 Vaccines and melanoma. *Hematol. Oncol. Clin. North Am.* **28**, 559–569. (doi:10.1016/j.hoc.2014.02.008)
39. Van Elssen C *et al.* 2017 Noninvasive imaging of human immune responses in a human xenograft model of graft-versus-host disease. *J. Nucl. Med.* **58**, 1003–1008. (doi:10.2967/jnumed.116.186007)
40. Woodham AW *et al.* 2018 Nanobody-antigen conjugates elicit HPV-specific antitumor immune responses. *Cancer Immunol. Res.* **6**, 870–880. (doi:10.1158/2326-6066.CIR-17-0661)
41. Dougan M *et al.* 2018 Targeting cytokine therapy to the pancreatic tumor microenvironment using PD-L1-specific VHHs. *Cancer Immunol. Res.* **6**, 389–401. (doi:10.1158/2326-6066.CIR-17-0495)
42. Jailkhani N, Ingram JR, Rashidian M, Rickelt S, Tian C, Mak H, Jiang Z, Ploegh HL, Hynes RO. 2019 Noninvasive imaging of tumor progression, metastasis, and fibrosis using a nanobody targeting the extracellular matrix. *Proc. Natl Acad. Sci. USA* **116**, 14 181–14 190. (doi:10.1073/pnas.1817442116)

43. Ingram JR *et al.* 2017 PD-L1 is an activation-independent marker of brown adipocytes. *Nat. Commun.* **8**, 647. (doi:10.1038/s41467-017-00799-8)
44. Ingram JR *et al.* 2018 Anti-CTLA-4 therapy requires an Fc domain for efficacy. *Proc. Natl Acad. Sci. USA* **115**, 3912–3917. (doi:10.1073/pnas.1801524115)
45. Rashidian M *et al.* 2017 Predicting the response to CTLA-4 blockade by longitudinal noninvasive monitoring of CD8T cells. *J. Exp. Med.* **214**, 2243–2255. (doi:10.1084/jem.20161950)
46. Xie YJ *et al.* 2019 Nanobody-based CAR T cells that target the tumor microenvironment inhibit the growth of solid tumors in immunocompetent mice. *Proc. Natl Acad. Sci. USA* **116**, 7624–7631. (doi:10.1073/pnas.1817147116)
47. Heckler M, Dougan SK. 2018 Unmasking pancreatic cancer: epitope spreading after single antigen chimeric antigen receptor T-cell therapy in a human phase I trial. *Gastroenterology* **155**, 11–14. (doi:10.1053/j.gastro.2018.06.023)
48. Cingolani P, Platts A, Wang LL, Coon M, Nguyen T, Wang L, Land SJ, Lu X, Ruden DM. 2012 A program for annotating and predicting the effects of single nucleotide polymorphisms, SnpEff: SNPs in the genome of *Drosophila melanogaster* strain w1118; iso-2; iso-3. *Fly* (*Austin*) **6**, 80–92. (doi:10.4161/fly.19695)